

**Depth Dependent Roles of CH_4 , NH_4^+ and $\Sigma\text{H}_2\text{S}$ in the Oxygen
Consumption of Base Mine Lake, the pilot Athabasca Oil
Sands Pit Lake**

Depth Dependent Roles of CH_4 , NH_4^+ and $\Sigma\text{H}_2\text{S}$ in the Oxygen Consumption of Base Mine Lake, the pilot Athabasca Oil Sands Pit Lake

By

PATRICK KEVIN MORRIS, B.Sc. (Hons).

A Thesis Submitted to the School of Graduate Studies in Partial Fulfilment of the Requirements for the Degree

Master of Science

McMaster University © Copyright by Patrick Kevin Morris, 2017

Master of Science (2017)

McMaster University

(Geography and Earth Science)

Hamilton, Ontario, Canada

Title: Depth Dependent Roles of CH_4 , NH_4^+ and $\Sigma\text{H}_2\text{S}$ in the Oxygen
Consumption of Base Mine Lake, the pilot Athabasca Oil Sands
Pit Lake

Author: Patrick K. Morris, B. Sc. (Honours)
McMaster University

Supervisor: Dr. Lesley Warren

Number of Pages: 82

Lay Abstract

Operators in the Athabasca Oil Sands Region of Canada (AOSR) produce millions of m³ of waste known as fluid fine tailings (FFT). A wet reclamation strategy currently being piloted by Syncrude Canada Ltd. to deal with these large volumes of tailings is water capped tailings technology (WCTT) in the form of a pit lake (PL), Base Mine Lake (BML). BML was built in an exhausted open pit mine, covering a layer (~40m) of FFT with a ~10m freshwater cap. For WCTT to be successful, a freshwater ecosystem capable of supporting life must develop within the water cap. As FFT contains compounds which can consume oxygen if mobilized into the water cap, there is uncertainty as to whether WCTT will be a successful FFT reclamation strategy. This thesis aimed to characterize oxygen consuming processes occurring throughout the water cap and revealed depth dependent importance of methane, ammonia and hydrogen sulfide in determining water cap oxygen concentrations.

Abstract

Extraction processes in the Athabasca Oil Sands Region of Canada (AOSRC) produce large volumes of tailings waste that require management and reclamation. Water capped tailings technology (WCTT) is currently being assessed as a reclamation strategy by Syncrude Canada Limited in the form of Base Mine Lake (BML), as it is the first AOSRC demonstration WCTT project (Fort McMurray, AB). BML is a pit lake (PL) consisting of a ~40 m layer of fluid fine tailings (FFT) that is capped with a ~10 m mixture of fresh and oil sands process waters. For BML to be considered a reclamation success, it should be able to support macrofauna; i.e. an oxic zone must develop and persist within the water cap. It is important to identify redox biogeochemical processes that influence oxygen concentrations in this pilot PL demonstration system to inform the design of the ~30 pit lakes (PL) that are currently planned across the AOSRC to ensure reclamation success.

To identify the oxygen consuming constituents (OCC) and the biogeochemical processes impacting BML oxygen concentrations, this study comprehensively characterized the water cap geochemistry using standard aquatic sampling methods over the summer of 2016, as well as using a specialized sampling device capable of capturing simultaneous samples every 10 cm over a 2-meter zone (n=20). The Fixed-Interval Sampler (FIS) was used to retrieve simultaneous samples in identified biogeochemically active zones of the metalimnion and hypolimnion- FFT-water interface (FWI) during the summer of 2016.

Seasonal results identified depth dependent concentration trends consistent with the FFT acting as a source of oxygen consuming constituents (OCC) to the overlying water cap. Characterized concentrations of CH_4 , NH_4^+ and $\Sigma\text{H}_2\text{S}$ were highest in the surface FFT pore water at $\sim 450\mu\text{M}$, $\sim 250\mu\text{M}$ and $\sim 25\mu\text{M}$, respectively, subsequently decreasing by the metalimnetic region to concentrations $<20\%$ of their respective hypolimnion-FWI concentrations, consistent with redox biogeochemical cycling and the observed profile of decreasing oxygen concentrations with increasing depth. Characterization of FIS samples provided greater resolution of trends specifically within the FWI region and the metalimnion. Results show that $\Sigma\text{H}_2\text{S}$ extinguishes rapidly above the FFT, reaching non-detectable concentrations by 1m above the FWI. Methane concentrations also decreased rapidly from $\sim 450\mu\text{M}$ in the FFT to $\sim 100\mu\text{M}$ by 0.3m above the FWI, consistent with methanotrophy. Characterization of FIS samples for nitrogen species concentrations within both the FWI and metalimnetic regions identified a near 1:1 conversion from NH_4^+ to NO_3^- by the metalimnion consistent with microbial nitrification. This process has not been shown to occur in oil sands tailings ponds, indicating that WCTT conditions can enable divergent biogeochemical cycling from that occurring in active tailings ponds. Evidence suggests that the relative concentrations of CH_4 and O_2 in the lower BML hypolimnion limit the ability of ammonia oxidizing microbes to carry out the full two-step nitrification process. This study has revealed the key oxygen consuming processes within the metalimnion and hypolimnion of BML and provides evidence that BML exhibits a difference in the relevance and magnitude of biogeochemical processes than those observed in tailings ponds. As such, tailings pond

research cannot be solely relied upon to determine the viability of PL as a successful reclamation strategy and further PL research is required to develop robust WCTT reclamation strategies.

Acknowledgements

My time pursuing a Master's degree at McMaster University was aided by a number of individuals, many of whom played a vital role in the successful completion of this thesis. First and foremost, I would like to thank my supervisor, Dr. Lesley Warren, for her ongoing guidance and encouragement throughout my 2 years here at McMaster University. Thank you for your patience, inspiration and continued belief in my ability as a researcher.

To all the members of the Aquatic Microbial Geochemistry Research Group, I want to thank you for your advice, knowledge and tolerance the past 2 years as I made the transition to this group of impressive young scientists. A heartfelt thank you to Tara Colenbrander-Nelson for her continued efforts in teaching me proper field and laboratory techniques as well as her help with countless field based logistical matters. To Florent and Daniel, a sincere thank you for your help in field sample collection. Also, a special mention to Florent for your patience in teaching me how to code in R and to make publishable figures.

I would like to acknowledge the entire Syncrude Canada, Mildred Lake Environmental Team for their help and support during my two summers in Fort McMurray. Specifically, Richard Kao and Chris Beierling, thank you for your positivity and welcoming nature, you two made summers in Fort McMurray a great time! Janna Lutz and Mohammed Salem, for their continued effort and assistance on site to ensure my project was running on time and with little setbacks. A big thank you to Dr. Matt Lindsay of the University of Saskatchewan for letting me use his Fixed-Interval Sampler, without you this project would not have been possible.

I am unbelievably grateful to my family for their unconditional love and support during these past two years. Thank you for listening to my presentations and providing positive feedback even though you weren't 100% sure what exactly my project was about. I could not have done this without you.

Lastly, I would like to acknowledge Syncrude Canada Ltd, NSERC and COSIA for funding this research.

Table of Contents

Lay Abstract	iv
Abstract	v
Acknowledgements	viii
Table of Contents	ix
List of Figures	xii
List of Tables	xiv
List of Abbreviations and Symbols	xv
1.0 Introduction	1
1.1 Sulfur Cycling in Oil Sands Tailings Ponds	6
1.1.1 Sulfate Reduction	6
1.1.2 Sulfide Oxidation	9
1.1.3 Sulfur Cycling in an Oil Sands Pit Lake	10
1.2 Methane in Oil Sands Tailings Ponds	11
1.2.1 Methanogenesis	11
1.2.2 Methanotrophy	13
1.2.3 Methane in an Oil Sands Pit Lake	14
1.3 Nitrogen Cycling in Oil Sands Tailings Ponds	15
1.3.1 Ammonia Oxidation	16
1.3.2 Nitrate Reduction	18
1.3.3 Nitrogen Cycling in an Oil Sands Pit Lake	19
2.0 Research Scope	21
2.1 Objectives	22
3.0 Methodology	24
3.1 Field Site Location and Description	25
3.2 Weekly Sampling Campaigns July -September 2016	27

3.3 Fixed Interval Sampler (FIS)	29
3.4 Physico-chemical Characterization of the BML Water Cap	32
3.5 Geochemical Analyses: Weekly Sampling (7 Depths throughout the BML Water Cap	33
3.5.1 $\Sigma\text{H}_2\text{S}$ Analysis	33
3.5.2 $\text{Fe}^{2+}/\text{Fe}^{3+}$ Analysis	33
3.5.3 NH_4^+ Analysis	34
3.5.4 NO_2^- Analysis	34
3.5.5 NO_3^- Analysis	35
3.5.6 SO_4^{2-} Analysis	35
3.5.7 CH_4 Analysis	35
3.6 FIS Geochemical Analyses	36
3.6.1 CH_4 Collection	36
3.6.2 $\Sigma\text{H}_2\text{S}$ Analysis	37
3.6.3 $\text{Fe}^{2+}/\text{Fe}^{3+}$ Sampling	38
3.6.4 SO_4^{2-} , NH_4^+ , NO_2^- , NO_3^- Sampling	39
3.6.5 Cleaning the FIS/Retrieving a Sample Blank	39
3.6.6 Statistical Analyses	40
4.0 Results and Discussion	41
4.1 2016 BML Water Cap Physico-chemical Zonation	42
4.2 2016 Summer BML OCC Trends	46
4.3 Water Column Physico-chemistry (FIS August 9 th and 16 th)	52
4.4 Metalimnetic and Hypolimnetic High Resolution FIS Geochemical Characterization: August 9 th , 16 th 2016	54
4.5 Hypolimnetic and Metalimnetic OCC vs Oxygen Concentration Relationships	58
4.6 Nitrification within the BML water cap	60
4.7 Competition between Methanotrophs vs. Ammonia Oxidizers	67

4.8 $\Sigma\text{H}_2\text{S}$, NH_4^+ and CH_4 Contribution to Oxygen Depletion in the BML hypolimnion/FWI	69
5.0 Conclusion	72
6.0 References	75

List of Figures

Figure 1.1	Potential biogeochemical cycles and physical factors occurring in BML	5
Figure 1.2	Sulfur cycling in a tailings pond/pit lake	8
Figure 1.3	Methane cycling in a tailings pond/pit lake	13
Figure 1.4	Potential nitrogen cycling in a pit lake	17
Figure 3.1	Map of Alberta and BML	26
Figure 3.2	Schematic of BML showing summer stratification	27
Figure 3.3	Sampling van Dorn used in summer 2016	29
Figure 3.4	Fixed-Interval Sampling: screwing on HDPE bottles	31
Figure 3.5	Fixed- Interval Sampling: evacuation of HDPE bottles	32
Figure 3.6	Sampling station on boat for Fixed-Interval Sampler	37
Figure 3.7	Specialized boat used for Fixed-Interval Sampler	38
Figure 4.1	Mean summer 2016 depth profile of temperature at P1	43
Figure 4.2	Mean summer 2016 depth profile of dissolved oxygen (%) at P1	43
Figure 4.3	Boxplots of 2016 (n=6) summer weekly geochemical data of $\Sigma\text{H}_2\text{S}$ and CH_4	49
Figure 4.4	Boxplots of 2016 (n=6) summer weekly geochemical data of NH_4^+ , NO_2^- and NO_3^- .	50

Figure 4.5	Temperature profiles of the BML water cap on both days of FIS sampling	52
Figure 4.6	Dissolved oxygen (%) profiles of the BML water cap on both days of FIS sampling	53
Figure 4.7	FIS generated OCC geochemical data of the BML water cap metalimnetic (n=20; red) and hypolimnetic-FWI (n=20; blue) zones	57
Figure 4.8	Linear regression models of FIS CH ₄ concentrations (n=20) versus oxygen in the metalimnetic and hypolimnetic-FWI region (b)	59
Figure 4.9	Linear regression models of FIS NH ₄ ⁺ concentrations (n=20) versus oxygen in the metalimnetic and hypolimnetic-FWI region (b)	60
Figure 4.10	Stacked bar chart depth profiles of total nitrogen species concentrations for FIS (a), as well as the weekly geochemical sampling data surrounding the FIS sampling, August 4 (b) and August 13 (c)	62
Figure 4.11	Stacked bar chart of relative proportion depth profiles of nitrogen species for FIS (a), as well as the weekly geochemical sampling data surrounding the FIS sampling, August 4 (b) and August 13 (c)	63
Figure 4.12	High resolution linear regression modelling of NH ₄ ⁺ conversion to NO ₂ ⁻ in the metalimnion (red; a) and hypolimnion (blue; b)	65

Figure 4.13	High resolution linear regression modelling of NO_2^- conversion to NO_3^- in the metalimnion (red; a) and hypolimnion (blue; b)	67
Figure 4.14	High resolution linear regression modelling of CH_4 vs. NH_4^+ conversion to NO_2^- in the metalimnion (red; a) and hypolimnion (blue; b)	68
Figure 4.15	Schematic of the mass balance calculations used to determine $\Sigma\text{H}_2\text{S}$ impact on BML O_2	70
Figure 4.16	Schematic of the mass balance calculations used to determine NH_4^+ impact on BML O_2	70
Figure 4.17	Schematic of the mass balance calculations used to determine CH_4 impact on BML O_2	71

List of Tables

Table 4.1	2016 physicochemical summary of weekly geochemical data	44
Table 4.2	Summary of BML geochemistry for the 2016 field season	51
Table 4.3	Dissolved Oxygen profiles in mg/L on both days the FIS was sampled	53

List of Abbreviations & Symbols

AOSRC – Athabasca Oil Sands Region of Canada

BML – Base Mine Lake

FFT – Fluid Fine Tailings

FWI – FFT-Water Interface

WCTT – Water cap tailings technology

OCC – Oxygen Consuming Constituents

OSPW – Oil Sands Processed Water

FIS – Fixed Interval Sampler

H₂S – Hydrogen Sulfide

SO₄²⁻ - Sulfate

CH₄ – Methane

NH₄⁺ - Ammonium

NO₂⁻ - Nitrite

NO₃⁻ - Nitrate

Fe²⁺ - Iron (II)

Fe³⁺ - Iron (III)

O₂ - Oxygen

Chapter 1 - Introduction

1.0 Introduction

The Athabasca Oil Sands Region of Canada (AOSRC) is home to approximately 170 billion barrels of recoverable bitumen that can be found within a mixture of clay, water, and sand (Pramanik, 2016; Ramos-Padrón et al., 2011). During the hot water extraction process of bitumen from these deposits, approximately 400,000 m³ of fluid fine tailings (FFT) are produced per day (Ramos-Padrón et al., 2011). This scale of FFT production translated to ~1.075 billion m³ of FFT in 2014 and has the potential to rise to 1.2 billion m³ by 2030 (Alberta Environment & Parks, 2016). In addition to the clay, water, and sand mixture, FFT include several toxic compounds including naphthenic acids and BTEX (Benzene, Toluene, Ethylbenzene and Xylenes) (Collins et al., 2016; Dompierre et al., 2016; Mohamad Shahimin et al., 2016; Stasik & Wendt-Potthoff, 2014). Prior to reclamation, FFT and impacted water are stored on site in basins known as tailings ponds. Currently, operators do not release tailings pond water to the environment and instead reuse this water in the extraction process, thereby limiting the fresh water to be taken from the Athabasca River (Siddique et al., 2012, 2007). As companies must return mined-out land back to the provincial government in a state of equivalent capability compared to the pre-mined environment (i.e. forests, wetlands, lakes), there is a need to identify environmentally safe and efficient approaches for FFT reclamation.

Currently, there are both wet and dry pilot FFT reclamation strategies being assessed in the AOSRC. Syncrude Canada Ltd. has implemented dry reclamation strategies, which include hydraulic sand capping on their Mildred Lake site. This approach has proven effective for reclaiming composite tailings (CT), a mixture of FFT

and gypsum, added to enhance consolidation (BGC Engineering, 2010). Furthermore, in the AOSRC, Syncrude Canada Ltd. is the first oil company to construct a commercial scale pit lake (PL) known as water capped tailings technology (WCTT) as a wet reclamation strategy for FFT (BGC Engineering, 2010; CEMA, 2007). Base Mine Lake (BML) was built in an exhausted open-pit mine that was filled with 40m of FFT (over ~17 years) and then capped with a ~10m layer of oil sands processed water (OSPW) and freshwater mixture (Dompierre et al., 2016). This PL was commissioned in December 2012 meaning that no further inputs of FFT have occurred since. The goal of WCTT is that some portion of the PL water cap eventually evolves into an ecosystem capable of supporting life (BGC Engineering, 2010; CEMA, 2007; Syncrude, 2017). For the PL to be considered a success it must develop and maintain an oxic water layer. Preliminary laboratory experiments and test pond results have shown this to be a promising technology (Syncrude, 2017), and so Syncrude Canada Ltd. have implemented a comprehensive monitoring strategy of the full scale demonstration, BML, to investigate the physical/chemical/biological factors that will influence oxygen concentrations within the water cap, as this will be a critical factor in enabling macrofauna to establish and persist in a AOSRC PL.

Previous studies on the biogeochemistry of AOSRC tailings ponds have identified key potential challenges associated with using WCTT as a reclamation strategy for FFT. The mobilization of oxygen consuming constituents (OCC) from the FFT may be sufficient to prevent the establishment of an oxic water layer in BML. Indeed, both CH_4 and $\Sigma\text{H}_2\text{S}$ have been widely documented to consume oxygen within tailings ponds (Chen

et al., 2013; Harner et al., 2011; Holowenko et al., 2000; Penner & Foght, 2010; Ramos-Padrón et al., 2011; Stasik & Wendt-Potthoff, 2014). Thus, within a PL they are hypothesized to be two of the main factors driving oxygen consumption within the water column (figure 1; BGC Engineering, 2010; CEMA, 2007). While NH_4^+ is abundant and released from FFT in tailings ponds (Holowenko et al., 2000), its contribution to observed oxygen decreases in tailings ponds has been negligible when compared to the impact of CH_4 and $\Sigma\text{H}_2\text{S}$ (Saidi-Mehrabad et al., 2012; Stasik et al., 2014). The current hypothesis as to why the microbially catalyzed oxidation of NH_4^+ to NO_2^- and ultimately to NO_3^- , has not been evident in AOSRC tailings ponds is that naphthenic acids (NA) toxicity has prevented the establishment of this process (40-120mg/L; Headley & McMartin, 2004; Quagraine et al., 2005; Rogers et al., 2002). This is because it has been demonstrated that NA concentrations $\geq 80\text{mg/L}$ can inhibit nitrification in an aerobic heterotrophic/nitrifying culture (Misiti et al., 2013). However, unlike a tailings pond, BML has a finite amount of FFT and over time may decrease NA concentrations $< 80\text{mg/L}$, potentially allowing nitrifying microbes to establish themselves. As such, NH_4^+ must be investigated as a potential key OCC.

Physical factors in BML will have a central role in determining where the most intense redox biogeochemical cycling will occur, with one of two main possible scenarios ensuing (Figure 1.1).

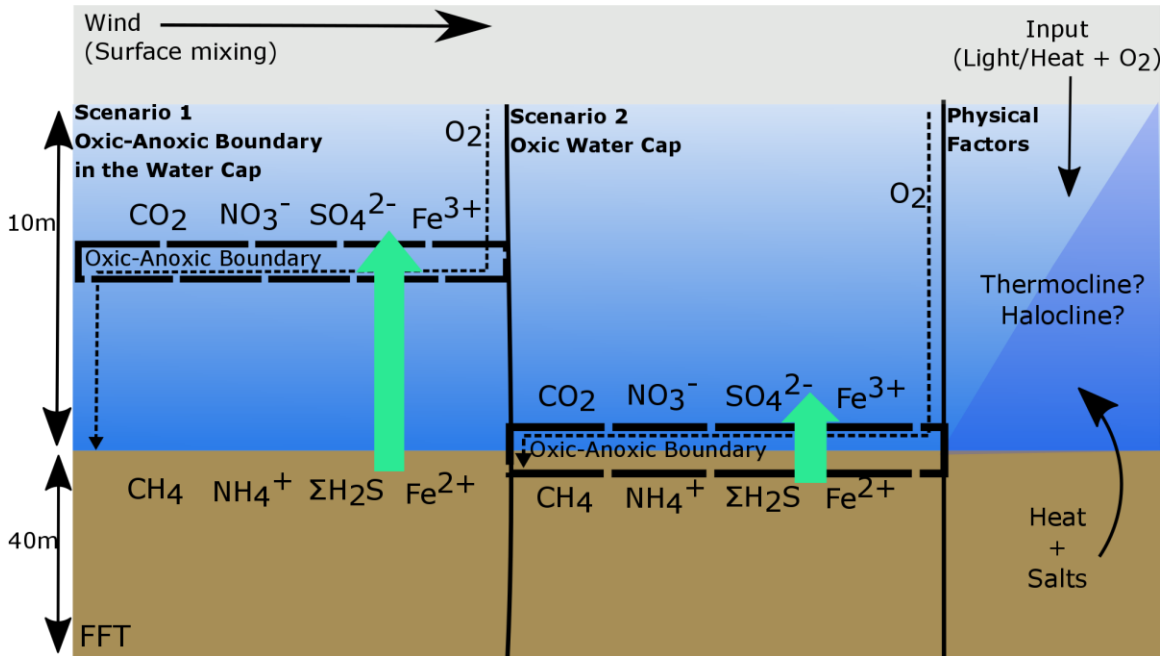


Figure 1.1- Schematic of the potential biogeochemical cycling that may occur in BML based on known potential oxygen consuming constituents (OCC) occurring within FFT, and associated with water cap physical factors that influence the location and extent of this cycling.

Scenario 1 results in an oxidic-anoxic boundary within the water cap of BML, not unlike that which has been shown to occur in tailings ponds (Ramos-Padrón et al., 2011; Stasik et al., 2014). With heat and salts being released from FFT associated with dewatering processes, BML's ability to thermally stratify and/or turnover is uncertain (CEMA, 2007). The input of heat from both the top (via the sun) and bottom (FFT dewatering) of the BML water cap may result in a weak or non-existent thermal stratification (CEMA, 2007; Lawrence et al., 2016). As such, aqueous OCC may be able to consume dissolved oxygen throughout the water cap into shallower waters over time as

they are not impeded by a density gradient. This would result in a shallow oxic zone (~1m) overlying a larger anoxic zone down to the FFT (~9m), making it difficult for macroscopic life to establish (Figure 1.1; Scenario 1). Alternatively, if BML were to have the oxic-anoxic boundary at the FFT-water interface (FWI) and thermally stratify, the separation of water layers by density may be able to constrain the OCC depletion of oxygen to the hypolimnion/FWI, allowing the upper water layers to remain oxygenated (Figure 1.1, Scenario 2).

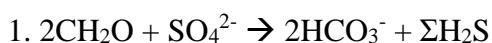
There are two main distinctions between a PL and a tailings pond, first, tailings ponds have a consistent input of fresh FFT pumped in on a daily basis as well as a shallower water cap. Further, tailings ponds consist of OSPW which is far more alkaline and higher in salinity than freshwater (Dompierre et al., 2016). While both PL and tailings ponds contain a layer of FFT capped with a water layer, their distinctions may generate physicochemical and biogeochemical discrepancies between the two. As such, to understand the biogeochemical processes affecting oxygen within a PL, the important biogeochemical cycles that contribute to oxygen consumption which derive from FFT principally in tailings ponds must be discussed.

1.1 Sulfur Cycling in Oil Sands Tailings Ponds

1.1.1 Sulfate Reduction

Sulfate, or SO_4^{2-} , is the most oxidized form of sulfur with an oxidation state of +6. SO_4^{2-} reduction involves the coupling of the reduction of sulfate with the oxidation of labile organic matter, in this case a general CH_2O molecule is used (equation 1). Sulfate-

reducing bacteria (SRB) thrive in anoxic environments where SO_4^{2-} and organic carbon are abundant. The oil sands ore mined by Syncrude Canada Ltd. are found in marine deposits containing elevated levels of sulfate in the formation water (+14 to +22‰ $\delta^{34}\text{S}$ as SO_4^{2-}) (King et al., 2014). Therefore, there are high levels of SO_4^{2-} introduced to the OSPW and FFT pore water during the extraction process (Masliyeh et al., 2008). While residual labile hydrocarbons are also in abundance in FFT, tailings ponds are an ideal environment for SRB (Holowenko et al., 2000; Stasik et al., 2014; Stasik & Wendt-Potthoff, 2014).



Microbial sulfate reduction is an important electron-accepting process for the decomposition of hydrocarbons in tailings ponds, potentially contributing to tailings pond detoxification (Harner et al., 2011; Holowenko et al., 2000; Stasik et al., 2014; Stasik & Wendt-Potthoff, 2014). However, the result of this microbial activity in the FFT is the release of large quantities of $\Sigma\text{H}_2\text{S}$ in to the water cap creating a high chemical oxygen demand partially contributing to the anoxia observed in tailings pond systems (figure 1.2) (Ramos-Padrón et al., 2011; Stasik & Wendt-Potthoff, 2014). While the release of $\Sigma\text{H}_2\text{S}$ from tailings ponds poses a risk to the surrounding environment, there is a potential benefit to promoting microbial sulfate reduction in FFT. By adding gypsum ($\text{CaSO}_4 \cdot \text{H}_2\text{O}$) to tailings ponds, FFT can consolidate at a faster rate because Ca^{2+} serves as a densification agent while the microbes reducing SO_4^{2-} simultaneously inhibit

methane production because sulfate reducers have a thermodynamic and kinetic advantage over methanogens (Arkell et al., 2015; Fedorak et al., 2003; Holowenko et al., 2000; Ramos-Padrón et al., 2011). An increase in densification rates will increase the amount of available water to recycle for the bitumen extraction process, decreasing the need for freshwater from the Athabasca river. Moreover, the potential ability to control methane production rates is important in tailings pond oxygen consumption and in the overall climate change context.

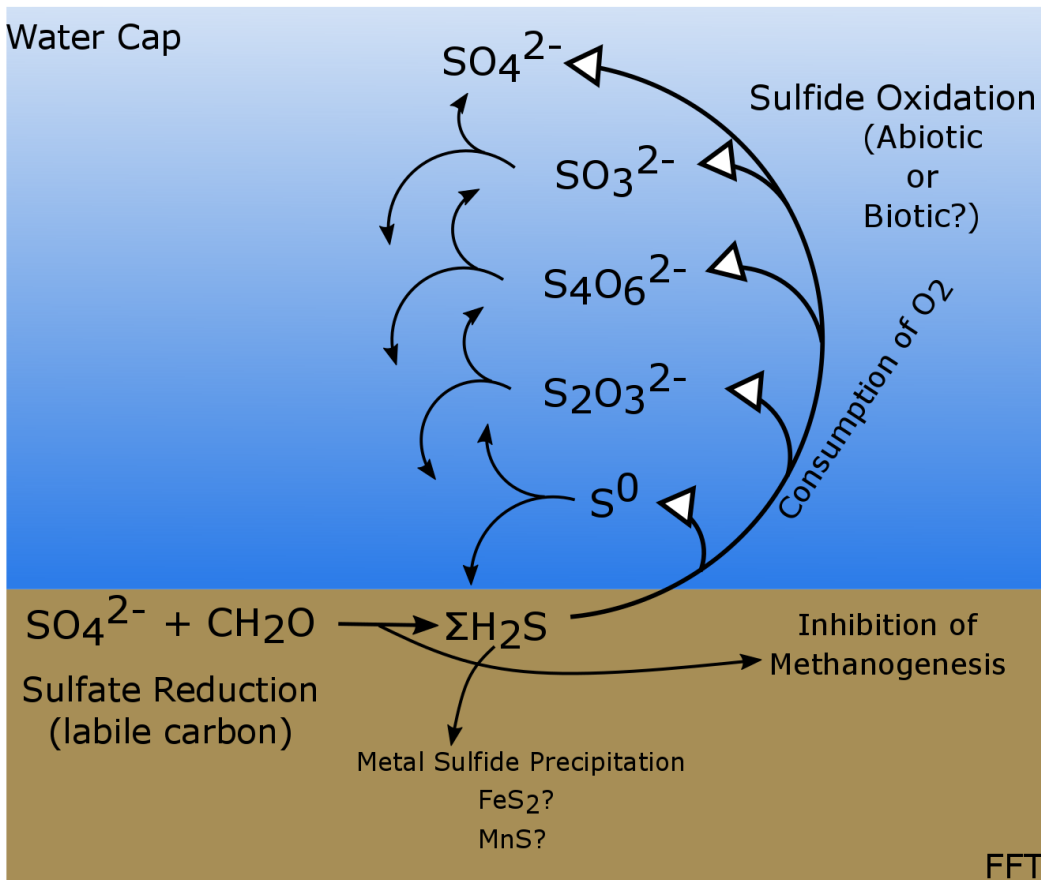


Figure 1.2- Schematic of sulfur cycling found within tailings ponds and what could potentially be expected to occur in a pit lake.

1.1.2 Sulfide Oxidation

Hydrogen Sulfide is the most reduced form of sulfur with an oxidation state of -2. Abiotic oxidation of $\Sigma\text{H}_2\text{S}$ happens quickly in the presence of oxygen around circumneutral pH, therefore microbes utilizing this metabolism must do so in low pH or microoxic conditions, i.e. acid mine drainage or sediment-water interfacial zones (Luther et al., 2011). Biotic oxidation of $\Sigma\text{H}_2\text{S}$ via sulfide-oxidizing bacteria (SOB), which are chemolithoautotrophs, oxidize $\Sigma\text{H}_2\text{S}$ using various electron acceptors (O_2 , NO_3^- , Fe^{3+} ; equation 2).



While there is potential for gaseous sulfide to be released in to the atmosphere from tailings ponds, it has been theorized that the $\Sigma\text{H}_2\text{S}$ produced by *in situ* microbial activity remains in the pond (Ramos-Padrón et al., 2011). Oil sands tailings ponds have continuous inputs of $\Sigma\text{H}_2\text{S}$ via FFT dewatering in to the water cap (Dompierre et al., 2016). In these ponds, at depths where oxygen is limited ($\sim 0.3 \mu\text{mol/g}$), $\Sigma\text{H}_2\text{S}$ can undergo either chemical or biological oxidation (Ramos-Padrón et al., 2011; Stasik et al., 2014; Stasik & Wendt-Potthoff, 2014). Some studies suggest biological oxidation is the more likely process, due to the high numbers of SOB found in tailings ponds (Chen et al., 2013; Ramos-Padrón et al., 2011; Stasik et al., 2014). This can result in many sulfur intermediate compounds being formed which can then be subsequently oxidized or reduced again in the water column, having further implications in both organic matter turnover and oxygen availability (Figure 1.2). Sulfide oxidation has been identified as

one of the major biogeochemical processes contributing to oxygen depletion in tailings ponds and is partially responsible for the large anoxic water column found in these systems (Ramos-Padrón et al., 2011; Stasik et al., 2014).

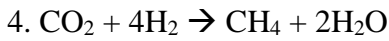
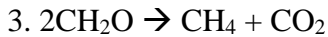
1.1.3 Sulfur Cycling in an Oil Sands Pit Lake

Sulfide oxidation is likely to be a key oxygen consuming process in PL, at least during the early stages (~5 years) given that heterotrophic SO_4^{2-} reduction is expected to occur in PL FFT pore water due to the understanding of its relevance in tailings ponds. However, given that PL have a finite amount of FFT with no input after commissioning, the extent to which SRB will thrive and whether over time the release of $\Sigma\text{H}_2\text{S}$ from the FFT will gradually decrease is unknown. Further, the ability of a PL to establish an oxic water layer will have implications as to where $\Sigma\text{H}_2\text{S}$ will be oxidized. An oxic water column down to the FFT will likely restrict $\Sigma\text{H}_2\text{S}$ oxidation to the FWI given the rapid abiotic oxidation kinetics. However, if the water cap is partially anoxic, then oxidation will occur wherever the oxic-anoxic boundary occurs, potentially depleting the O_2 found in surface layers of BML, which would be the important zone for macrofauna development (Holowenko et al., 2000; Ramos-Padrón et al., 2011). Additionally, without fresh input of FFT, it is likely that SO_4^{2-} will become depleted in the FFT pore water, thereby likely increasing the methanogenic potential of FFT resulting in a increased release of CH_4 (Ramos-Padrón et al., 2011; Stasik & Wendt-Potthoff, 2014).

1.2 Methane in Oil Sands Tailings Ponds

1.2.1 Methanogenesis

Methanogenesis refers to the production of methane via methanogens using either H₂ or acetate as their substrate, in this case CH₂O is used as the general organic carbon molecule (equations 3 and 4) (Garcia et al., 2000).



Methanogenesis via labile organic carbon (equation 3) is an important electron accepting process, alongside sulfate reduction, for the decomposition of organic matter and detoxification of tailings ponds (Garcia et al., 2000; Harner et al., 2011; Mohamad Shahimin et al., 2016; Siddique et al., 2012). As methanogenesis is an anaerobic process, found mainly in lake or marine sediments, it can only occur when most other electron acceptors are depleted (NO₃⁻, Fe³⁺, SO₄²⁻). This makes FFT an ideal environment for methanogens to thrive, as such, there are many studies documenting methane release from FFT and its impact on the surrounding environment (figure 1.3) (Arkell et al., 2015; Penner & Foght, 2010; Stasik et al., 2014; Stasik & Wendt-Potthoff, 2014).

Mildred Lake Settling Basin (MLSB), among other tailings ponds has a documented methane flux where, 60-80% of the flux of gas to the atmosphere across the basin is CH₄ (Holowenko et al., 2000). Studies have shown this amount of methane in MLSB is produced via both H₂ and acetate by methanogens and at one point released the equivalent of 0.5 million cows of CH₄ per day (12g/m²) (Holowenko et al., 2000; Ramos-

Padrón et al., 2011). These tailings ponds pose a risk to global climate change with the amount of methane they release daily, however there are also benefits in a PL scenario to the production of CH₄ in FFT. The processes by which the production of CH₄ occurs has been shown to increase the rate of settling of FFT, resulting in a more defined separation of the water cap from the FFT as well as a greater recovery of pore water that can be recycled to use again for bitumen extraction (Arkell et al., 2015; Fedorak et al., 2003; Siddique et al., 2014). While in a PL, the porewater will not be recycled, it will result in a deeper water cap potentially diluting the impact of OCC mobilized from the FFT. Further, a deeper water cap could increase the separation of upper water layers and contribute to the establishment of a macrofauna zone while the OCC continue to consume O₂ in the hypolimnion-FWI region.

While the methane production in FFT is substantial, several studies have shown that it can be inhibited by the activity of SRB due to competition for similar electron donors (H₂ and labile organic carbon; equations 3 + 4) (Fedorak et al., 2003; Holowenko et al., 2000; Ramos-Padrón et al., 2011; Salloum et al., 2002; Stasik & Wendt-Potthoff, 2014). While SRB have a thermodynamic and kinetic advantage over methanogens, the availability of SO₄²⁻ is integral in aiding this process. SO₄²⁻ concentrations in FFT pore water are low (~50µM; Ramos-Padrón et al., 2011; Stasik et al., 2014; Stasik & Wendt-Potthoff, 2014), so while this process may be observed in tailings ponds or laboratory experiments, it is likely this inhibition will only be possible for a certain period of time in a PL given there are no fresh inputs of FFT (i.e. SO₄²⁻).

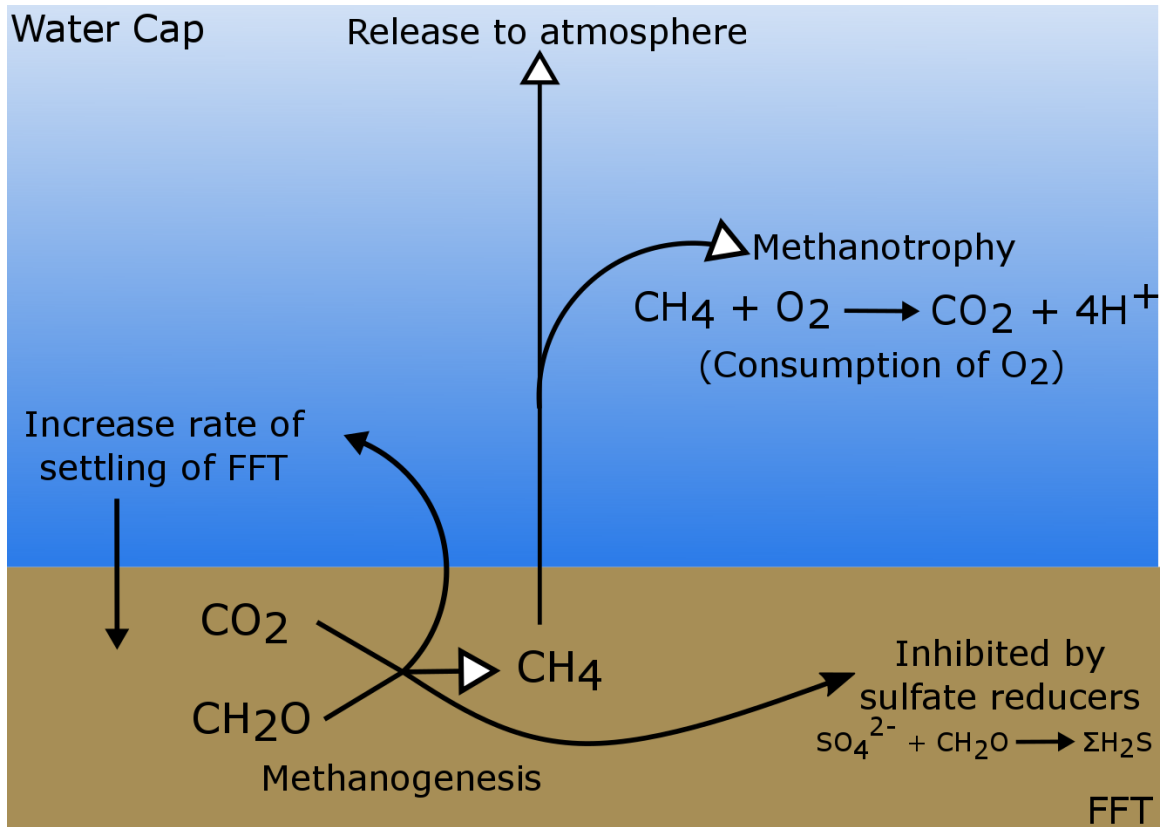
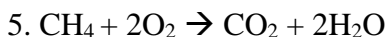


Figure 1.3- Simplified schematic of methane cycling and its implications in an oil sands tailings pond. These processes have the potential to occur in a pit lake.

1.2.2 Methanotrophy

Methanotrophy refers to the oxidation of methane via microbial metabolism (equation 5). Aerobic methane oxidation is found where oxygen and methane meet, this includes ponds, lakes, marine sediments and hydrothermal vents (Torres-Alvarado et al., 2005). Aerobic methanotrophy has the ability to consume high amounts of methane in a small layer where oxygen concentrations are high (Carini et al., 2005). The oxic-anoxic interface of aquatic systems is where there is the potential for the highest rates of methanotrophy to occur.



Methanotrophy has been documented in oil sands tailings ponds as one of the main drivers of oxygen depletion alongside sulfide oxidation (Holowenko et al., 2000; Saidi-Mehrabad et al., 2012; Stasik et al., 2014; Stasik & Wendt-Potthoff, 2014). Aqueous methane is introduced into the anoxic water column of tailings ponds and consumes O_2 once it reaches the oxic-anoxic boundary. CH_4 concentrations observed in tailings pond water caps range from 45-3400 μM (Holowenko et al., 2000), while rates of methanotrophy in tailings ponds have been documented from 75-150 $\text{nmol mL}^{-1} \text{day}^{-1}$ in the surface waters (Saidi-Mehrabad et al., 2012) which is within the range of natural lake ecosystems (Carini et al., 2005; Bastviken et al., 2002).

1.2.3 Methane in an Oil Sands Pit Lake

Certainly, methane cycling is going to be important in the overall PL biogeochemistry due to the magnitude of CH_4 release from the underlying FFT to the water column above (Dompierre et al., 2016; Mohamad Shahimin et al., 2016; Siddique et al., 2011). Methanogenesis and/or legacy concentrations in the FFT makes CH_4 mobilization possible via dewatering and diffusion (Dompierre et al., 2016; Mohamad Shahimin et al., 2016). Once CH_4 gets into the overlying water column, there is potential for it to be converted by aerobic heterotrophs (equation 5) and contribute to anoxia (CEMA, 2007; Fedorak et al., 2003; Mohamad Shahimin et al., 2016; Siddique et al., 2012). If BML were to stratify with an oxic water layer, it is possible that methanotrophic depletion of oxygen will be restricted to the FWI allowing the upper water layers to

remain oxygenated. However, if BML does not stratify, it is likely that methanotrophy will contribute to the creation of an anoxic water cap with a shallow (~1m) oxic layer near the surface as seen in tailings ponds (Saidi-Mehrabad et al., 2012; Stasik et al., 2014). Furthermore, the extent to which methanotrophy will occur in BML is currently unknown because while FFT in tailings ponds release large amounts of CH₄ (12 g/m²) (Holowenko et al., 2000; Ramos-Padrón et al., 2011), BML does not have a continuous input of fresh FFT, which may lead to lower amounts of CH₄ released in to the water column over time. However, the timeline in which this may happen is unknown and low oxygen levels in the water column may prevent the establishment of a viable lake ecosystem for many years. Additionally, with methanogenesis inducing a faster rate of the settling of FFT, over several years the water cap will become deeper, which may in turn influence stratification patterns creating a deeper water column resulting in a slower rate of turnover (Boehrer & Schultze, 2008; Dompierre et al., 2016).

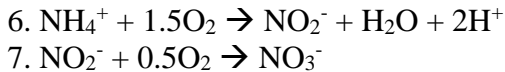
1.3 Nitrogen Cycling in Oil Sands Tailings Ponds

Studies have consistently demonstrated that although NH₄⁺ is abundant and widespread throughout tailings ponds, nitrification does not contribute to the oxygen depletion found in these systems (Harner et al., 2011; Saidi-Mehrabad et al., 2012; Stasik et al., 2014). However, NH₄⁺ may be important in a PL scenario as NH₄⁺ will still be high in parent FFT and the factor thought to inhibit microbial nitrification, i.e. naphthenic acid toxicity, in oil sands tailings ponds (Misiti et al., 2013; Quagraine et al., 2005), may be reduced enabling nitrifying microbes to establish and impact oxygen concentrations

within the PL water cap (Saidi-Mehrabad et al., 2012; Stasik et al., 2014). As such, nitrogen cycling in a PL may be an important process affecting water cap oxygen concentrations.

1.3.1 Ammonia Oxidation

The process known as nitrification, occurs when NH_4^+ is oxidized to NO_2^- and eventually NO_3^- via microbes. This process is carried out by chemolithoautotrophs oxidizing NH_4^+ aerobically (Ramanathan et al., 2014). The first step of nitrification (equation 6) is a six electron transfer carried out by aerobic bacteria, and then followed by the second step (equation 7) where the terminal oxidized species NO_3^- , is produced.



Nitrifiers need oxygen to thrive, although sometimes only a small amount is required (1-6 μM), these types of conditions are present at the oxic-anoxic interface of stratified lakes where oxygen from the top layers meets with NH_4^+ from the anoxic sediments. As previously mentioned, NH_4^+ is abundant in tailings ponds (~10mg/L; 700 $\mu\text{mol/L}$) throughout the water column (Stasik et al., 2014). Though tailings ponds have conditions suitable for the oxidation of NH_4^+ to occur, it has not been found to play an important role in tailings pond oxygen consumption (Arnell et al., 2015; Collins et al., 2016; Saidi-Mehrabad et al., 2012). This is most likely because concentrations of NA >80mg/L are toxic to nitrifying organisms, and with tailings pond NA concentrations

ranging from 40-120mg/L, it is possible that NA toxicity is impeding nitrifiers in these systems (Headley & McMartin, 2004; Misiti et al., 2013; Quagraine et al., 2005; Rogers et al., 2002).

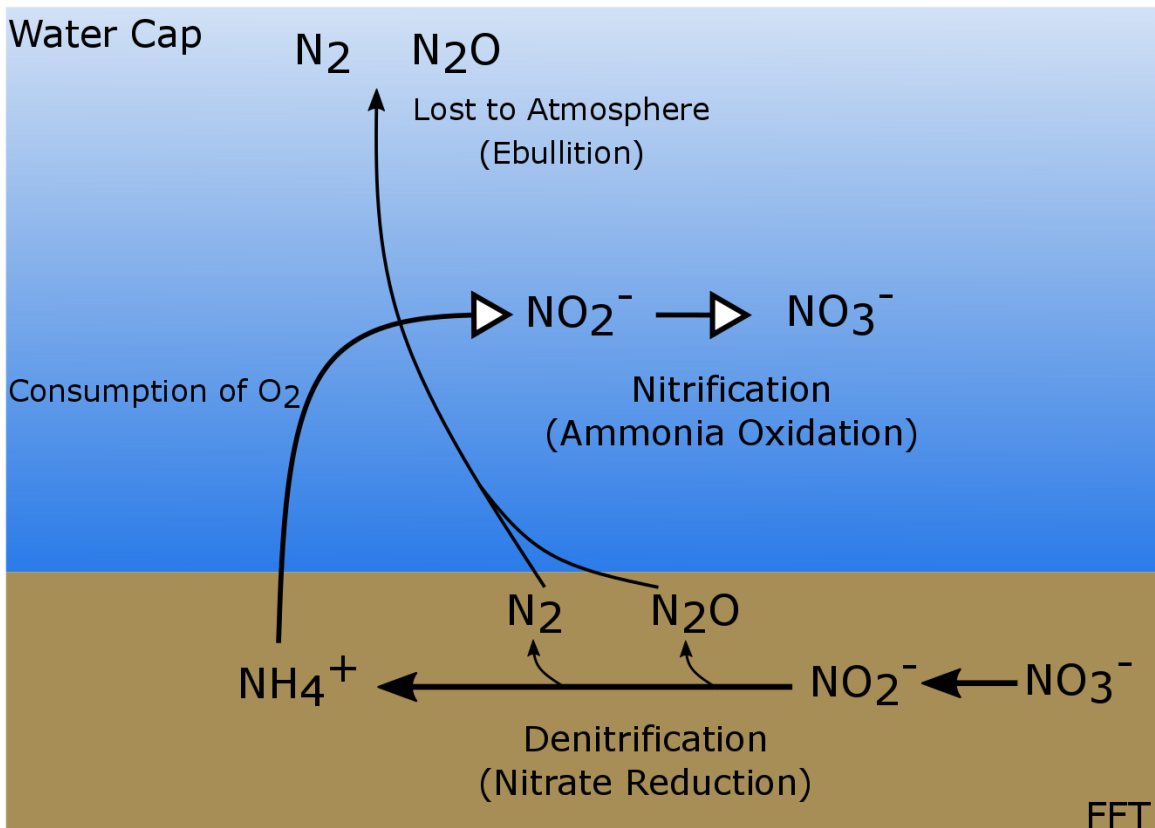
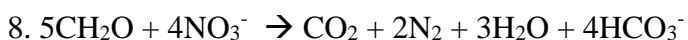


Figure 1.4- simplified schematic of nitrogen biogeochemistry that could potentially be found in an oil sands pit lake.

1.3.2 Nitrate Reduction

Nitrate, NO_3^- , exists in a +5 oxidation state and can be reduced via a process known as denitrification. Most microbes that carry out nitrate reduction are anaerobic heterotrophs utilizing labile carbon such as acetate, in this case depicted as CH_2O (equation 8), while others use H_2 as their electron donor. These microbes thrive just below the oxic zone of sediments and can also be found in the oxygen depleted zones of lake hypolimnia (Tiedje, 1988).



Denitrifiers thrive under anoxic conditions where labile carbon and NO_3^- are abundant. Though studies have shown low concentrations ($<0.04\text{mg/L}$) of NO_3^- in tailings pond samples (Stasik et al., 2014; Stasik & Wendt-Potthoff, 2014) nitrate reducers were found to be present in MLSB (Harner et al., 2011; Holowenko et al., 2000). However, NO_3^- reduction has been ruled out as an important process in hydrocarbon degradation because of its uncommon detection in petroleum reservoirs (Harner et al., 2011). Yet, this cannot be assumed to occur in a PL scenario, and if NO_3^- reducing bacteria were to become relevant it could lead to becoming a major factor in organic matter turnover as well as a regeneration of NH_4^+ possibly leading to a continuous depletion of oxygen throughout the PL water cap.

Further, the process of denitrification can produce both N_2 and N_2O gas which can leave the system via ebullition (Figure 1.4, equation 6). While this has not been

documented to occur in tailings ponds it may be an issue in the future of PL. The loss of nitrogen via ebullition may result in less bioavailable nitrogen in the future, which could affect the ability of macroscopic flora and fauna to establish in this ecosystem.

To sustain microbial life in tailings ponds, sufficient bioavailable nutrients must be present. Collins et al., (2016) showed that N_2 fixation occurred in conjunction with methanogenesis in mature fine tailings cultures amended with a labile carbon source, suggesting the possibility of N_2 fixing microbes *in situ*. This may be an important process in the future of PL as organisms will need bioavailable nitrogen in the system.

1.3.3 Nitrogen Cycling in an Oil Sands Pit Lake

As previously discussed, NA toxicity may impede the establishment of nitrifying organisms in tailings ponds, however unlike a tailings pond, PL have a finite amount of FFT and over time through microbial degradation, may have NA concentrations low enough for nitrifying microbes to establish.

With ammonia mobilized from the FFT and having high concentrations ($\sim 700 \mu\text{mol/L}$) in a tailings pond water cap, NH_4^+ will also be expected to mobilize to a certain degree in a PL (Collins et al., 2016). If NA toxicity is an issue in BML, it is likely there will be relatively high concentrations of NH_4^+ throughout the water cap, similar to those found in tailings ponds. If NA toxicity is not an issue in a PL, the ability of the system to stratify as well as where the oxic-anoxic boundary is found will influence where nitrification will occur. A BML water column that does not stratify will result in NH_4^+ moving up the water column consuming oxygen in consistently shallower waters until a large portion of the water column becomes anoxic, just as the other OCC

discussed. However, a stratified BML water column may be able to constrain NH_4^+ oxidation to the hypolimnion, allowing the upper water layers to remain oxygenated.

Chapter 2- Research Scope

2.0 Research Scope

Syncrude Canada Ltd. have built a pilot scale PL, Base Mine Lake, to test the viability of WCTT for wet reclamation of FFT that if successful, provides the capability to permanently store and reclaim millions of m³ of FFT while simultaneously becoming a viable ecosystem capable of sustaining macroscopic life. The viability of this WCTT for all operators in the AOSRC will represent an important milestone in FFT reclamation as ~40 more PL are planned to be constructed throughout the region, if this pilot PL is demonstrated to have success (BGC Engineering, 2010; CEMA, 2007). The biogeochemical cycles of sulfur and carbon have been demonstrated to negatively impact oxygen concentrations observed in oil sands tailings ponds, with evidence that sulfate reduction and methanogenesis are key drivers in organic matter turnover and oxygen consumption. As BML is the first full scale demonstration PL, a comprehensive understanding of the biogeochemical processes contributing to oxygen consumption within the lake is paramount in the future success of WCTT.

2.1 Objectives

The field-based objectives of this thesis are to:

- 1) characterize the BML summer biogeochemistry through sequential (Van Dorn) and simultaneous (Fixed-Interval Sampler) sampling approaches, specifically in the biogeochemically active zones of the metalimnion and hypolimnion-FWI.

- 2) identify key OCC responsible for driving any observed oxygen loss found within the BML water cap.

Chapter 3- Methodology

3.0 Methodology

3.1 Field Site Location and Description

Field sample collection for geochemical data occurred during July-September 2016 within the vicinity of the main sampling platform located in the approximate middle of BML (figure 3.1). BML, the oil sands first demonstration PL is located ~35km north of Fort McMurray, AB on the Mildred Lake Mine site on the Syncrude Canada Ltd. lease (figure 3.1). The mine lease covers ~1000km², which is considered to be one of the largest worldwide (Carey, 2008). The regional climate is sub-humid continental which results in cold winters and warm summers. BML was commissioned in December 2012 and is the first of its kind in the AOSRC. It was built in an exhausted open-pit mine where FFT was slowly deposited over ~17 years to a depth of ~40m, then capped with ~10m of a mixture of oil sands processed water (OSPW) and freshwater pumped in via Beaver Creek Reservoir (BCR) (figure 3.2).

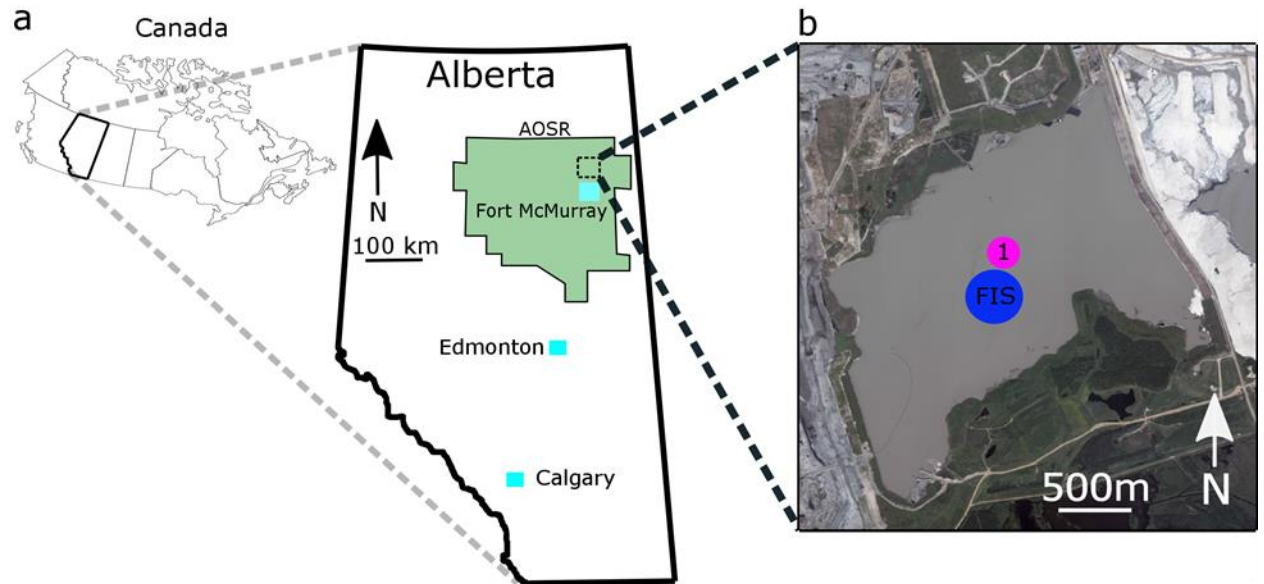


Figure 3.1- a; map depicting the location of Fort McMurray, Alberta. b; map of BML showing the location of the P1 and where the FIS sampling took place.

BCR inputs are regulated and monitored constantly to make sure fish and other aquatic organisms do not reach BML. Water is withdrawn from BML to simulate a natural flowthrough; withdrawn water is reused in the extraction process. The inflow and outflow rates are balanced to keep the surface water elevation constant.

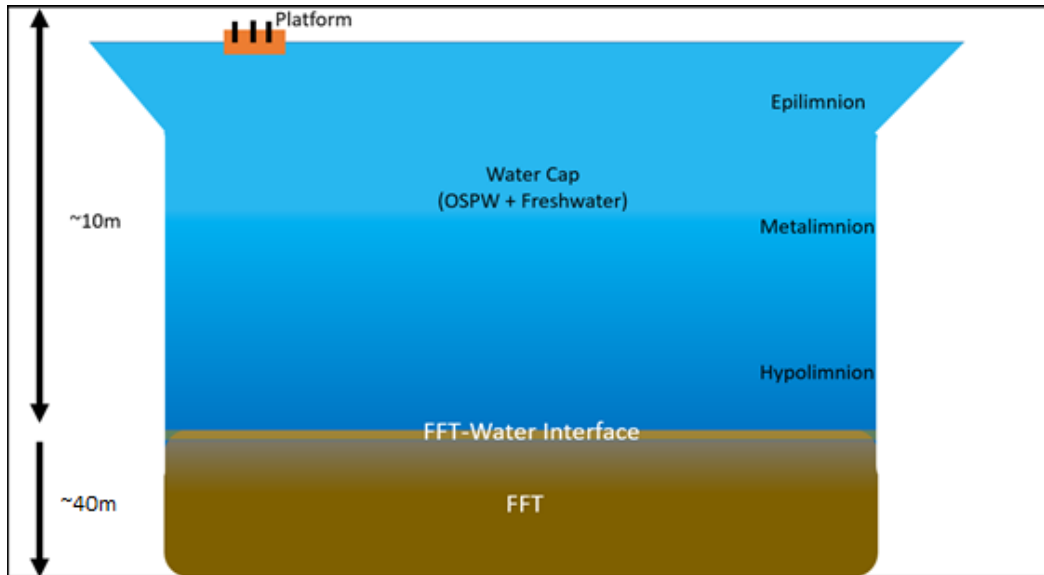


Figure 3.2- schematic of BML showing summer stratification and separation of layers. The FFT is slowly dewatering, so every year the FFT layer gets smaller and the water cap deepens.

The future plan for BML is that it will be connected to the surrounding watershed and eventually connect with the other closure landscapes on Syncrude Canada's land and to the Athabasca river (CEMA, 2007). BML covers $\sim 8\text{km}^2$ and is directly adjacent to Highway 63.

3.2 Weekly Sampling Campaigns July-September 2016

Sampling efforts in the summer of 2016 were initially postponed as a result of the Fort McMurray wildfire that took place in May 2016. With initial plans to sample from May to September it was not until July when McMaster students were allowed back on site. Once back, armed with knowledge of 2015 data which showed no statistically

significant differences amongst the three sampling platforms (Risacher et al., 2017), our samplings efforts were focused on P1, in the center of BML. Every week, for a total of 8 sampling campaigns, 1-2 days were dedicated to collecting samples at 7 depths throughout the water column for the weekly geochemical data (1x air-water interface, 1x epilimnion, 2x metalimnion, 2x hypolimnion, 1x FFT-water interface).

Weekly geochemical samples were retrieved using a van Dorn (figure 3.3), which was lowered to each of the 7 desired depths and then brought to the surface to sample, preserve and analyze redox species in the following order: CH_4 , $\Sigma\text{H}_2\text{S}$, Fe, NH_4^+ , NO_2^- , NO_3^- and SO_4^{2-} . All sample preservation and analyses followed well-established protocols developed in our research groups as described in section 3.5 (Reid and Warren, 2016; Warren et al., 2016; Slater, 2008; Risacher et al., 2017). Overall, all sampling containers and equipment used for the sampling campaign or analysis in the lab were previously acid cleaned in 5% v/v solution for ~12 hours and then rinsed 7 times with ultra-pure ($18.2\Omega\text{m cm}^{-1}$, milli-Q, Millipore) water in order to ensure all trace inorganic analytes were gone.



Figure 3.3- the sampling Van Dorn used in summer 2016 for weekly geochemical data sampling.

3.3 Fixed Interval Sampler (FIS)

High resolution fixed-interval sampling occurred over two days: August 9, 2016 and August 16, 2016 at platform 1 (P1) in the metalimnetic and hypolimnetic- FFT- water interfacial zones (figure 3.2). Similarly, as with the weekly geochemical data, to establish the depths over which high resolution samples (10 cm intervals over a 2 meter depth zone simultaneously) were to be collected, a Sonde (YSI Professional Plus 6-Series Sonde, YSI Incorporated) was first used to determine the metalimnetic and FWI zones within the BML water cap. All sample preservation and analysis followed what will be discussed in the geochemical analysis section (section 3.5). Sample collection however, differs.

250mL High density polyethylene (HDPE) bottles were placed in a 5% HCL (v/v) solution and rinsed 7x with ultra-pure ($18.2\Omega\text{m cm}^{-1}$, milli-Q, Millipore) water to ensure all trace inorganic analytes are gone. Once on the boat ConeTec employees helped with the proper operation and sample retrieval with the pneumatic piston sampler. To begin, the device was lowered to the desired depth via a winch and left sitting for 20 minutes to ensure the least amount of disturbance of the water column and retrieve the most representable samples of the zone. Samples at depth were then drawn in to the sampler using a pressure activated pneumatic piston, once the piston was fully drawn back, the ball valve closed and the sampler was retrieved (Dompierre et al., 2016). Samples were then immediately transferred to 5% HCl clean 250mL HDPE bottles (figure 3.4). Subsequently, the sampler was placed horizontally on the boat and the sample in each chamber was forced out in to the HDPE bottles via a pressure activated system (figure 3.5).

Because the FIS did not allow our team to collect samples the same way as the van Dorn had allowed us to, we needed to change our sampling approach while simultaneously aware of the redox sensitive species (CH_4 , $\Sigma\text{H}_2\text{S}$ and $\text{Fe}^{2+}/\text{Fe}^{3+}$). These three species were sampled/ preserved directly on the boat immediately following sample retrieval as described subsequently in Section 3.6.



Figure 3.4- As the FIS was drawn up one sample chamber at a time, HDPE bottles were screwed on to minimize sample loss.



Figure 3.5-The sampler had to be placed horizontally to ensure all water sample chambers were properly evacuated and the pressure system did not force the HDPE bottles off of the threading.

3.4 Physico-chemical Characterization of the BML Water Cap

For each sampling campaign, the depth to the FWI was found using a Castaway-CTD (Version 1.5). Immediately following, field measurements of pH, dissolved oxygen (% saturation, mg/L), ORP, NTU, temperature (°C), and specific conductivity ($\mu\text{S}/\text{cm}$) were collected at every 0.5m from the BML surface to the FWI using a YSI (YSI Professional Plus 6-Series Sonde, YSI Incorporated). The YSI sonde was cleaned and calibrated regularly in order to ensure accurate measurements were being taken in the field.

3.5 Geochemical Analyses: Weekly Sampling (7 depths throughout the BML water cap)

3.5.1 $\Sigma\text{H}_2\text{S}$ Analysis

$\Sigma\text{H}_2\text{S}$ analyses using the methylene blue method (Method 8131) were done immediately on the boat in order to ensure none was oxidized. Sample was collected by syringing 30 mL of sample directly from the closed van Dorn via the embedded sampling tube, using a 3-way stop cock into a 60 mL plastic syringe, then filtered through a 0.45 μm sterile syringe filter on the boat. Sample was syringed into 15mL tubes containing reagents to fix the $\Sigma\text{H}_2\text{S}$ and analyzed by the methylene blue method using a HACH portable spectrophotometer (Hach DR/2800 spectrophotometer, HACH Company, Loveland, CO, USA).

3.5.2 $\text{Fe}^{2+}/\text{Fe}^{3+}$ Analysis

Iron species were immediately preserved once the sample was collected in the Van Dorn using 2% (v/v) Optima grade HCl in 2x14mL of sample directly on the boat. These samples were then stored at 4°C until laboratory analyses could be done at McMaster University. The method was taken from (Viollier et al., 2000) where 100 μL of ferrozine reagent solution was added to 1mL of sample and the first absorbance was recorded at 562nm (3x replicates). 300 μL was then removed from the sample cuvette and 150 μL of hydroxylamine hydrochloride solution was added. Then cuvette was then covered and left to react for 10 minutes. Immediately following this, 50 μL of the third reagent (ammonium acetate buffer) was added and the second absorbance was recorded

for all three replicates. This process was repeated for both filtered and unfiltered BML samples throughout the water cap. All samples were compared to a corresponding standard curve for iron species with a correlation (R^2) of 0.99 or higher.

3.5.3 NH_4^+ Analysis

NH_4^+ analysis was done with a spectrophotometer using method 10031 no later than a week after the sample was collected. <24 h following sample collection, it was filtered using a 0.45 μm filter and stored at 4°C in the dark to ensure no further microbial activity. Three replicates of 10mL (1/5 diluted) had ammonia salicylate (reagent 1) added to them, shaken and then left to react for three minutes. Ammonia cyanurate (reagent 2) was then added, shaken and left for 15 minutes for the reaction to take place. Replicates were then analyzed and values recorded.

3.5.4 NO_2^- Analysis

NO_2^- analysis was done using a spectrophotometer following the USEPA diazotization method 8507 in replicates of three. <24 h following sample collection it was filtered using a 0.45 μm filter and stored at 4°C in the dark to ensure bacteria would not manipulate the sample. Three replicates of 10mL (1/2 diluted) had NitriVer 3 reagent added to them, shaken and left to react for 20 minutes. Replicates were then analyzed and values recorded.

3.5.5 NO₃⁻ Analysis

NO₃⁻ analysis was done using a spectrophotometer following the “Cadmium reduction method” 8171 in replicates of three. 0-1 days following sample collection it was filtered using a 0.45µm filter and stored at 4°C in the dark to ensure bacteria would not manipulate the sample. Three replicates of 10mL (1/2 diluted) had NitraVer 6 added, vigorously shaken for 1 minute and then left for 5 minutes for the reaction to complete. Replicates were then analyzed and recorded.

3.5.6 SO₄²⁻ Analysis

SO₄²⁻ analysis was done using a spectrophotometer following the USEPA SulfaVer 4 method 8051 in replicates of three. 0-1 days following sample collection it was filtered using a 0.45µm filter and stored at 4°C in the dark to ensure bacteria would not manipulate the sample. Three replicates of 10mL (1/5 diluted) had SulfaVer 4 added, swirled and then left for 5 minutes for the reaction to complete. Replicates were then analyzed and recorded.

3.5.7 CH₄ Analysis

CH₄ was extracted immediately upon retrieval of the sampling van Dorn on the boat, by syringing 30 mL of sample directly from the closed van Dorn via the embedded sampling tube, using a 3-way stop cock into a 60 mL plastic syringe. The water was then transferred by injection into a pre-evacuated 60 mL serum bottle crimp-sealed with a one cm blue buytl septa. Septa had been pretreated by boiling in 1 molar NaOH for one hour prior to evacuation of the bottles. Bottles were pre-loaded with mercuric chloride to halt

any further microbial activity after sampling. Samples were stored refrigerated and subsequently analyzed upon return to McMaster University by Dr. Greg Slater's lab and specifically Corey Goad (Goad et al., 2017).

3.6 FIS Geochemical Analyses

3.6.1 CH₄ Analysis

Immediately following the unscrewing of the 250mL bottle from the FIS (figure 3.5), the sample was capped and brought over to the sampling table (figure 3.6). Once at the sampling table, the lid from the HDPE bottle was unscrewed and the designated syringe (by depth) was then used to transfer 30mL of sample by injection in to a pre-evacuated 60 mL serum bottle crimp-sealed with a 1 cm blue buytl septa. This was done for all 20 depths before moving on to the next redox species to be sampled. Samples were stored refrigerated and subsequently analyzed upon return to McMaster University by Dr. Greg Slater's lab and specifically Corey Goad (Goad et al., 2017).



Figure 3.6- the sampling table for the FIS. Each depth had it's own syringe, needle and bottle to make sure there was no cross contamination when handling 20 samples at once.

3.6.2 $\Sigma\text{H}_2\text{S}$ Analyses

Due to limited space and time allotted on the FIS sampling boat (figure 3.8), the procedure for sampling $\Sigma\text{H}_2\text{S}$ was changed. 30mL of the sample was still syringed and fixed with the appropriate reagents inside the 60mL syringe so that no $\Sigma\text{H}_2\text{S}$ was lost via oxidation. The sample syringes however, were then capped with syringes needles and placed in the dark at 4°C. Once the on-boat activities were completed for the day, upon return to the Mildred Lake Environmental Lab, the $\Sigma\text{H}_2\text{S}$ samples were immediately filtered using a 0.45 μm syringe filter and analyzed.



Figure 3.7- the specialized Fixed-Interval Sampling boat used for both FIS days in August.

3.6.3 Fe²⁺/Fe³⁺ Preservation and Analyses

Iron species were the final geochemical species to be sampled on the boat. With the limited water sample available, only 1 x14mL was able to be collected for dissolved and colloidal (14mL unfiltered + 14mL filtered). Using separate acid clean 60mL syringes for each depth, sample was transferred to 2% HCl (v/v) 15mL tubes and a 0.45µm sterile syringe filter was used for the filtered fraction sample collection. These samples were then analyzed via the method was taken from (Viollier et al., 2000) where 100µL of ferrozine reagent solution was added to 1mL of sample and the first absorbance was recorded at 562nm (3x replicates). 300µL was then removed from the sample cuvette and 150µL of hydroxylamine hydrochloride solution was added. Then cuvette was then

covered and left to react for 10 minutes. Immediately following this, 50 μ L of the third reagent (ammonium acetate buffer) was added and the second absorbance was recorded for all three replicates. This process was repeated for both filtered and unfiltered BML FIS samples. All samples were compared to a corresponding standard curve for iron species with a correlation (R^2) of 0.99 or higher.

3.6.4 SO_4^{2-} , NH_4^+ , NO_2^- , NO_3^- Sampling

With the limited water sample remaining (<150mL) for each depth, these remaining geochemical species were analyzed according to the previous methods put forth in the weekly geochemical sampling section (Section 3.5).

3.6.5 Cleaning the FIS/Retrieving a Sample Blank

As can be seen in the photos, the FIS is not very clean (on the outside) this is because it is primarily an FFT sample collector. As such, before my samples were taken, several cleaning steps were carried out to minimize contamination. First, the ConeTec team scrubbed the sampler to the best of their ability. Second, brake fluid was used to clean the inside of the of each chamber cell. Once this had been done, the FIS was placed in the surface of BML and rinsed 3x before use. A sample blank was retrieved on both August 9th and 16th, 2016 and subtracted from the FIS geochemical sampling data with respect to the day each was taken. The blank was retrieved by determining the “dirtiest” chamber on the FIS and filling it with ultra pure (18.2 Ω m cm^{-1} , milli-Q, Millipore) water and then sampled for all geochemical analytes.

3.6.6 Statistical Analyses

Differences in means of OCC were tested using ANOVAs to compare each species individually, separated by layer. A paired t-test was used to compare mean concentrations of species at the same depth but on different dates. Linear regressions were created to assess the relationship between oxygen concentrations (x axis) and ratios of OCC concentrations (y axis). All statistical analyses were performed and figures created using R studio (version 1.0.136, RStudio Inc, 2016) working with R base (version 3.3.1, R Development Core Team, 2016) and Excel 2016.

Chapter 4- Results and Discussion

4.0 Results and Discussion

4.1 2016 BML Water Cap Physico-chemical Zonation

As evident from Figure 4.1, the BML water cap was thermally stratified during the summer of 2016. 2016 temperatures in the epilimnion reached a maximum of $\sim 22^{\circ}\text{C}$, while the greatest decrease was observed in the metalimnion, $\sim 5^{\circ}\text{C}$ over 2m, temperatures in the hypolimnion ranged between $13\text{-}14^{\circ}\text{C}$ (figure 4.1, Table 4.1). Oxygen concentration and saturation also showed clear zonation within the BML water cap, rapidly decreasing from an epilimnetic maxima of $\sim 7\text{mg/L}$ or $\sim 80\%$ saturation (Figure 4.2, Table 4.1) to a hypolimnetic minima at the FWI of $<0.4\text{mg/L}$ or $<5\%$ saturation over the 2016 summer season. The defined oxygen stratification pattern observed at P1 over the summer of 2016 is likely due to the FFT settling, introducing OCC in to the water cap and subsequently oxidizing in the hypolimnion (Arkell et al., 2015; Siddique et al., 2014). Consistent with the alkaline FFT produced through the extraction process, the BML water cap was circumneutral in pH (7.9-8.3), while salinity (1.51 ‰) and turbidity (150-250 NTU) typically evidenced higher values closer to the FWI (Table 4.1). Consistent with the oxygenated status of the BML water cap, ORP values ranged from ~ 93 in the epilimnion to 69 mV near the FWI (Table 4.1).

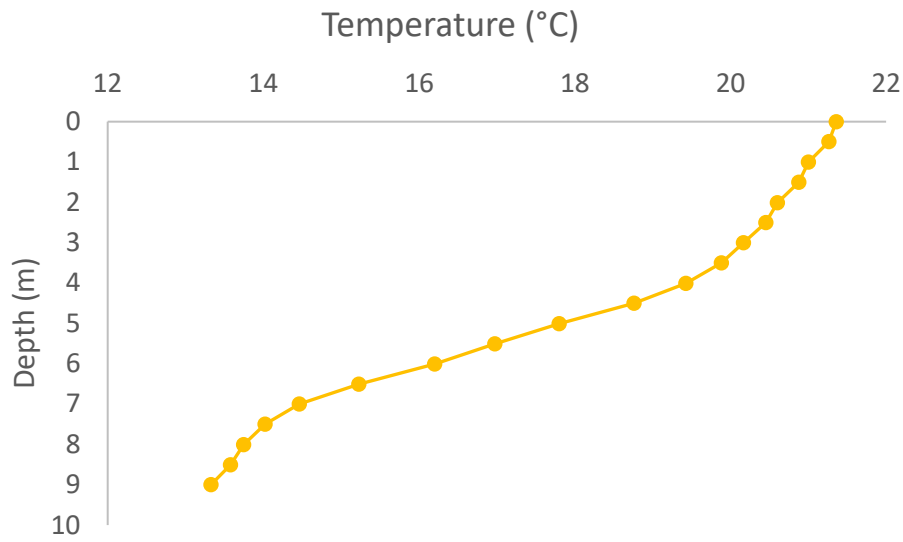


Figure 4.1- mean summer 2016 depth profile of temperature at P1 (July 3-August 14; n=6)

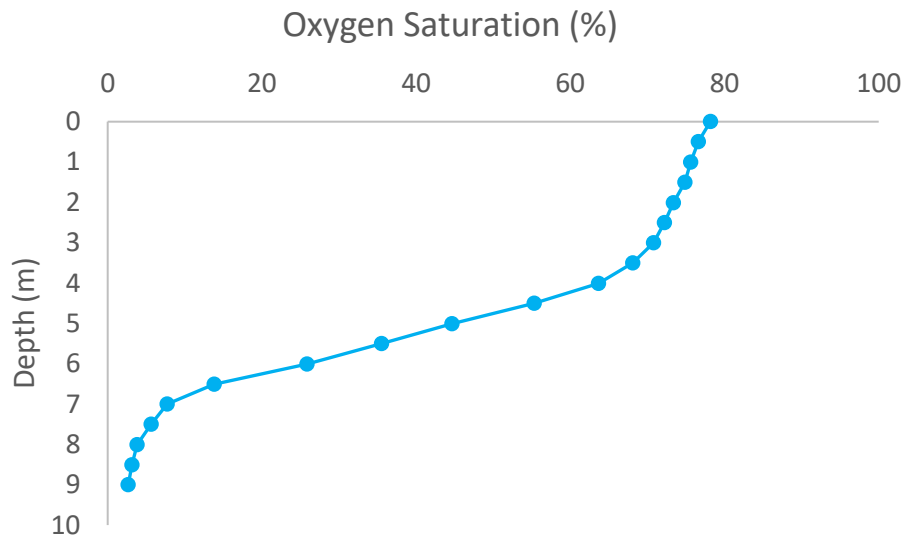


Figure 4.2- mean summer 2016 depth profile of oxygen saturation at P1 (July 3-August 14; n=6).

Table 4.1- 2016 temperature, dissolved oxygen, pH, ORP, turbidity and salinity from weekly sampling data of the entire summer (n=6) at each depth and in each zone.

Depth (m) / Zone	Temperature (°C)	DO (%)	DO (mg/L)	pH	ORP (mV)	Turbidity (NTU)	Salinity (‰)
0	21.3 ± 0.4	78 ± 2.2	6.8 ± 0.1	8.3 ± 0.001	98 ± 8	51 ± 3	1.46 ± 0.01
0.5	21.3 ± 0.5	77 ± 2	6.7 ± 0.1	8.4 ± 0.03	94 ± 8	52 ± 3	1.46 ± 0.01
1	21 ± 0.4	76 ± 1.8	6.7 ± 0.1	8.4 ± 0.03	93 ± 7	52 ± 3	1.46 ± 0.01
1.5	20.9 ± 0.3	75 ± 1.5	6.6 ± 0.1	8.4 ± 0.03	92 ± 7	53 ± 3	1.46 ± 0.01
2	20.6 ± 0.2	73 ± 1.1	6.5 ± 0.09	8.4 ± 0.04	91 ± 7	53 ± 3	1.46 ± 0.01
2.5	20.5 ± 0.2	72 ± 1.2	6.5 ± 0.09	8.3 ± 0.04	91 ± 6	53 ± 3	1.46 ± 0.01
3	20.2 ± 0.2	71 ± 0.8	6.4 ± 0.06	8.3 ± 0.04	92 ± 5	54 ± 4	1.46 ± 0.01
3.5	19.9 ± 0.3	68 ± 1.3	6.1 ± 0.09	8.3 ± 0.03	91 ± 5	57 ± 5	1.46 ± 0.01
4	19.4 ± 0.5	64 ± 2.9	5.8 ± 0.2	8.3 ± 0.03	91 ± 5	60 ± 7	1.47 ± 0.007

4.5	18.8 ± 0.5	$55 \pm$	$5.1 \pm$	$8.3 \pm$	$92 \pm$	45 ± 3	$1.47 \pm$
		3.1	0.3	0.03	5		0.005
5	17.8 ± 0.5	$45 \pm$	$4.2 \pm$	$8.2 \pm$	$94 \pm$	70 ± 9	$1.48 \pm$
		3.0	0.3	0.04	5		0.005
5.5	16.9 ± 0.6	$36 \pm$	$3.4 \pm$	$8.2 \pm$	$95 \pm$	79 ± 10	$1.48 \pm$
		4.3	0.4	0.06	5		0.006
6	16.2 ± 0.7	$26 \pm$	$2.5 \pm$	$8.1 \pm$	$96 \pm$	87 ± 10	$1.49 \pm$
		5.2	0.5	0.06	6		0.007
6.5	15.2 ± 0.4	$14 \pm$	$1.4 \pm$	$8.1 \pm$	$98 \pm$	108 ± 10	$1.5 \pm$
		5.1	0.5	0.07	6		0.006
7	14.4 ± 0.3	$7.7 \pm$	$0.8 \pm$	$8.0 \pm$	$97 \pm$	138 ± 7	$1.5 \pm$
		3.2	0.3	0.06	3		0.008
7.5	14 ± 0.2	$5.6 \pm$	$0.6 \pm$	$8.0 \pm$	$98 \pm$	143 ± 11	$1.51 \pm$
		2.2	0.2	0.07	6		0.01
8	13.7 ± 0.2	$3.7 \pm$	$0.4 \pm$	$8.0 \pm$	$64 \pm$	166 ± 16	$1.51 \pm$
		0.7	0.07	0.05	10		0.1
8.5	13.6 ± 0.2	$3.2 \pm$	$0.3 \pm$	$8.0 \pm$	$41 \pm$	170 ± 19	$1.52 \pm$
		0.3	0.03	0.06	13		0.02
9	13.3 ± 0.1	$2.6 \pm$	$0.3 \pm$	$8.0 \pm$	$37 \pm$	205 ± 25	$1.51 \pm$
		0.08	0.02	0.08	16		0.01
Epilimnion	20.6 ± 0.1	$73 \pm$	$6.5 \pm$	$8.3 \pm$	$93 \pm$	54 ± 3	$1.46 \pm$
		0.8	0.4	0.02	6		0.003

Metalimnion	17 ± 0.3	35 ±	3.4 ±	8.2 ±	95 ±	78 ± 8	1.48 ±
		3	0.3	0.03	7		0.003
Hypolimnion	14 ± 0.1	4.7 ±	0.5 ±	8.0 ±	69 ±	162 ± 11	1.51 ±
		0.9	0.09	0.02	15		0.008

Observed BML water cap epilimnetic oxygen concentrations were much higher than those observed in oil sands tailings ponds, i.e. 80% saturation in BML compared to 6.5% saturation at the surface in tailings ponds. Further, oxygen persists to the FWI in BML, albeit at low concentrations (<5% saturation), compared to tailings ponds where anoxia typically occurs below the first meter (Ramos-Padrón et al., 2011; Stasik et al., 2014).

4.2 2016 Summer BML OCC Trends

Results from the six 2016 weekly sampling campaigns (July 7th to Aug 13th, 2016) from the summer identified water column geochemical trends consistent with mobilization of OCC from the FFT layer as observed in 2015 (Risacher et al., 2017); i.e. high concentrations of $\Sigma\text{H}_2\text{S}$, CH_4 and NH_4^+ at the FWI decrease moving upwards into the epilimnion (Figures 4.3,4.4; Table 4.2). $\Sigma\text{H}_2\text{S}$ concentrations in 2016 (Figure 4.3a) exhibit detectable concentrations ranging from 0.5-6 μM close to the FFT and then below detection in the lower hypolimnion and above. This result is consistent with the oxygenated water cap and the potential for rapid abiotic oxidation of $\Sigma\text{H}_2\text{S}$ within the FWI (Luther et al., 2011; Roden, 2012). CH_4 concentrations at the FWI ranged between

10-140 μM (Goad, 2017; Figure 4.3b), and are similar to those observed in tailings ponds consistent with mobilization of legacy concentrations from the FFT and/or *in situ* production (Holowenko et al., 2000; Penner & Foght, 2010; Siddique et al., 2012). Once CH_4 reached the metalimnion and above, it's concentrations become trace ($<1\mu\text{M}$; Figure 4.3b; Table 4.2). Mean summer 2016 BML hypolimnetic NH_4^+ concentrations are much lower than those found in tailings ponds ($\sim 700\mu\text{M}$; Stasik et al., 2014) with concentrations of $\sim 45\mu\text{M}$ in the hypolimnion persisting through the water column to a mean value of $\sim 15\mu\text{M}$ in the epilimnion (Figure 4.4a; Table 4.2) consistently throughout the summer of 2016.

In contrast to geochemical trends for potential OCC mobilized from the FFT, concentrations of oxidized species of nitrogen show differing trends to those observed by the reduced counterpart. NO_2^- concentrations range between 0 and $10\mu\text{M}$ across depth and sampling campaigns in 2016 (Figure 4.4b), however there is no consistent trend with depth. In contrast, 2016 NO_3^- concentrations show a trend that is almost a complete reversal of 2016 NH_4^+ (Figure 4.4a,c; Table 4.2) where concentrations were lowest in the hypolimnion, closest to the FWI ($\sim 20\mu\text{M}$) and steadily increase throughout the water column reaching a mean value of $\sim 45\mu\text{M}$ in the epilimnion. This observed conversion of NH_4^+ to NO_3^- throughout the water cap is the first line of evidence to suggest the presence of nitrifying microbes in BML.

SO_4^{2-} concentrations were orders of magnitude higher than those observed for all other geochemical analytes, in the 1500-2500 μM range (Table 4.2), and show greater spatial and temporal variability with no consistent trend in depth profiles. Fe^{3+} concentrations were low and exhibit no consistent trends with depth over the 2016 field season with concentrations staying below 3 μM throughout the water cap (Table 4.2).

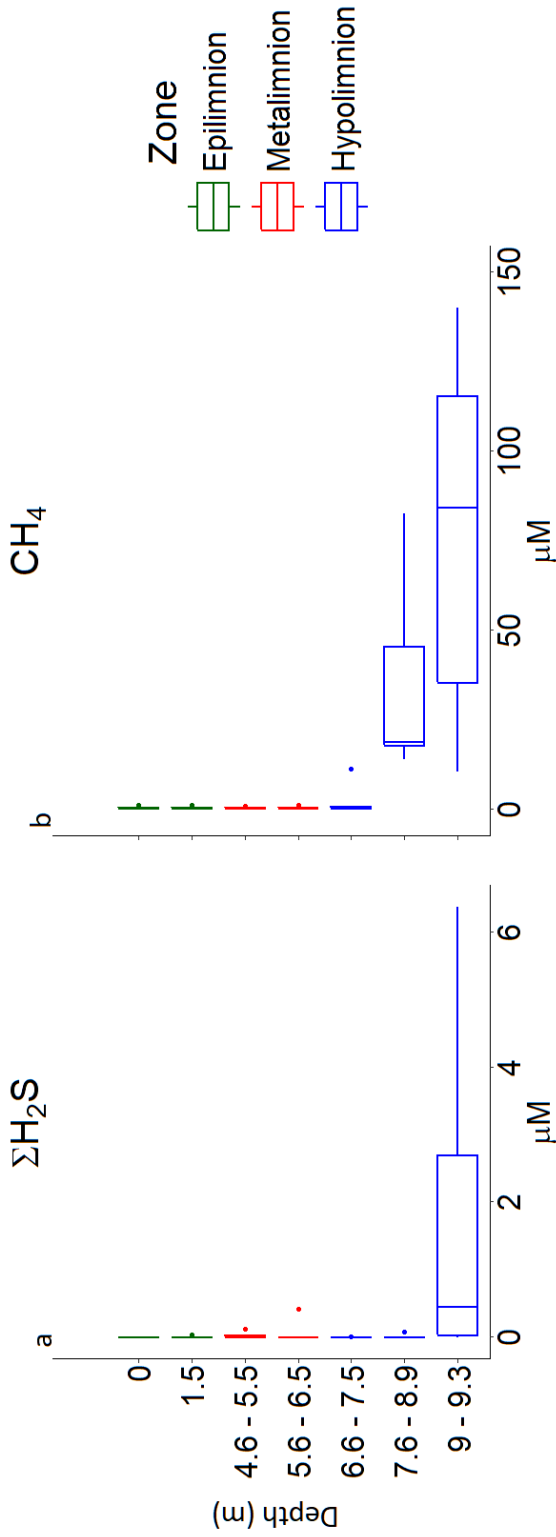


Figure 4.3- Boxplots of 2016 ($n=6$) summer weekly geochemical data of ΣH_2S and CH_4 . Boxplot whiskers represent the 0-25th and 75th-100th quartiles. The middle boxes represent the 25th-50th and 50th - 75th quartiles while the solid middle vertical line represents the median in the data. Solid dots represent outliers.

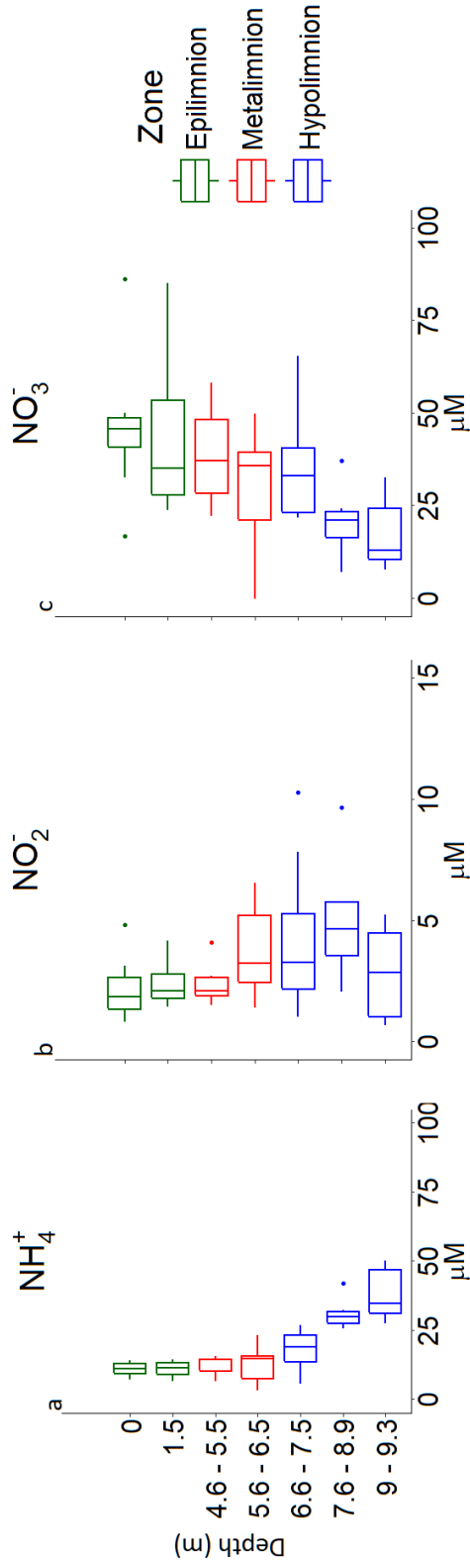


Figure 4.4- Boxplots of 2016 ($n=6$) summer weekly geochemical data of NH_4^+ , NO_2^- and NO_3^- . Boxplot whiskers represent the 0-25th and 75th- 100th quartiles. The middle boxes represent the 25th- 50th and 50th - 75th quartiles while the solid middle vertical line represents the median in the data. Solid dots represent outliers.

*Table 4.2- Summary of BML geochemistry for the 2016 field season. BDL = Below**Detection Limit*

Constituent	Epilimnion	Metalimnion	Hypolimnion
CH ₄ (μM)	0.45 ± 0.06	0.41 ± 0.09	26 ± 7
ΣH ₂ S (μM)	BDL	BDL	0.5 ± 0.3
NH ₄ ⁺ (μM)	11 ± 1	11 ± 2	27 ± 2
NO ₃ ⁻ (μM)	44 ± 5	40 ± 6	27 ± 3
NO ₂ ⁻ (μM)	2.3 ± 0.3	3.7 ± 0.6	5.0 ± 0.8
SO ₄ ²⁻ (μM)	2085 ± 65	2103 ± 104	2140 ± 56
Fe ²⁺ (μM)	0.04 ± 0.01	0.09 ± 0.04	0.09 ± 0.04
Fe ³⁺ (μM)	0.9 ± 0.3	2.8 ± 1.3	2.1 ± 0.9

2016 summer weekly geochemical results indicated that the FFT layer was a source of OCC to the overlying BML water cap and in particular identified that ΣH₂S was important at the FWI for oxygen consumption, while CH₄ was important within the FWI and hypolimnion (Figure 4.3). However, results also indicated a shift in nitrogen species between the hypolimnetic and metalimnetic zones indicating that ammonia oxidation was occurring (Figure 4.4).

4.3 Water Column Physico-chemistry (FIS August 9th and 16th)

The FIS sampling provided simultaneous high resolution geochemical characterization of both the FWI-lower hypolimnion and the metalimnetic regions (20 samples collected at 10cm intervals over a 2m region; collected August 9th and 16th 2016). Physicochemical profiles of temperature (Figure 4.5) and oxygen (Figure 4.6) for the two FIS sampling dates identify similar thermal and % DO saturation profiles.

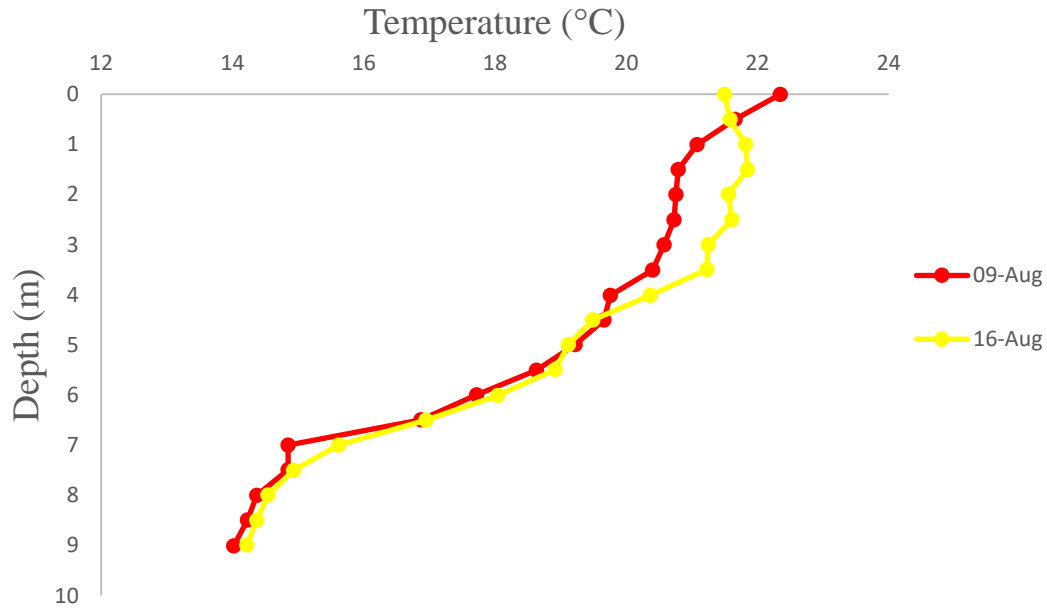


Figure 4.5- Temperature profiles of the BML water cap on both days the FIS was used. August 9th when the metalimnion was sampled (red). August 16th when the hypolimnion/FWI was sampled (yellow).

Based on the dissolved oxygen saturation profile from August 9th (Figure 4.6; table 4.3), it was decided to sample from 4.5m to 6.4m in the water column as this range of depth captured the largest decrease in O₂ over the metalimnion. Based on the dissolved oxygen saturation profile for August 16th (Figure 4.6; table 4.3) the hypolimnion/FWI

was sampled from 7.6m to 9.5m to capture the FWI and lower hypolimnion of BML, ensuring the ability to assess OCC mobilization from the FFT. As determined by the YSI Sonde and FIS, 9.5m was the surface FFT pore water, 9.4m was the depth of the FWI and 9.3m was within the overlying water cap.

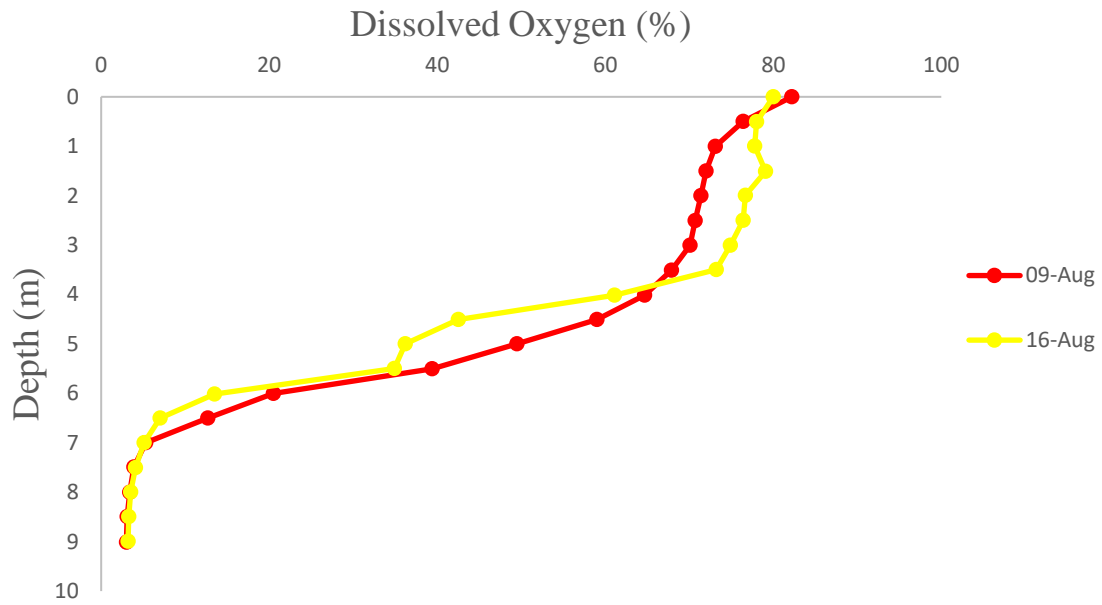


Figure 4.6- Dissolved oxygen (%) profiles of the BML water cap on both days the FIS was used. August 9th when the metalimnion was sampled (red). August 16th when the hypolimnion/FWI was sampled (yellow).

Table 4.3- Dissolved oxygen profiles in mg/L on both days the FIS was used

Depth (m)	Dissolved Oxygen (mg/L)	
	August 9 th 2016	August 16 th 2016
0	7.08	7
0.5	6.66	6.82
1	6.45	6.77
1.5	6.39	6.88

2	6.34	6.71
2.5	6.29	6.68
3	6.24	6.59
3.5	6.07	6.45
4	5.86	5.47
4.5	5.36	3.87
5	4.53	3.32
5.5	3.65	3.22
6	1.94	1.26
6.5	1.21	0.67
7	0.54	0.51
7.5	0.4	0.41
8	0.35	0.35
8.5	0.32	0.34
9	0.31	0.32

4.4 Metalimnetic and Hypolimnetic High Resolution FIS Geochemical Characterization: August 9th, 16th 2016

Geochemical results for CH_4 , NH_4^+ and $\Sigma\text{H}_2\text{S}$ from the FIS sampling of the metalimnetic region (Depth 4.5 to 6.4m) are shown in Figure 4.7a, b and c, while those collected from the hypolimnetic region (Depth 7.6 to 9.5m) are shown in Figure 4.7d, e and f. For comparison, the values characterized for depths contained within each of these 2m regions for these three parameters from the August 4th and August 13th weekly sampling campaigns using the van Dorn bottle are also shown. CH_4 , NH_4^+ and $\Sigma\text{H}_2\text{S}$ concentrations in the metalimnion are <20% of those observed in the hypolimnion

(Figure 4.5a, b, c). NH_4^+ was the only OCC to have concentrations higher than trace levels in the upper water layers ($\sim 10\mu\text{M}$; figure 4.7b). Concentrations detected at the same depth in the metalimnion for CH_4 , NH_4^+ and $\Sigma\text{H}_2\text{S}$ from the van Dorn (August 4th; 4.5m, 6m and 6.5m) are not significantly different from the FIS data collected at the same depths (August 9th; T-test, d.f. = 2, $p > 0.05$) with the exception of NH_4^+ at 6.5m (August 9th, T-test, d.f. = 2, $p < 0.05$).

Further, concentrations detected at the same depth in the hypolimnion for CH_4 and NH_4^+ from the van Dorn (August 13th; 7.5m, 8m and 9.3m) are significantly different from the FIS data collected at the same depths (August 16th; T-test, d.f. = 2, $p < 0.05$). $\Sigma\text{H}_2\text{S}$ only exhibits 9.3m as being significantly different (August 16th, T-test, d.f. = 2, $p < 0.05$) while 7.5m and 8m reveal the same concentrations between both sampling techniques used (August 16th, T-test, d.f. = 2, $p > 0.05$). Although hypolimnetic concentrations for all three OCC detected by the van Dorn and FIS reveal significant statistical differences, which is to be expected given different sampling techniques used on different days, the trends between the van Dorn and FIS data collected are similar. As such, data collected via the FIS is reliable.

In BML, within the first 30cm above the FFT, CH_4 decreased significantly (ANOVA, d.f.=2, $p < 0.05$) from $\sim 500\mu\text{M}$ in the surface FFT to $\sim 100\mu\text{M}$ just above the FFT in the water cap and reached trace concentrations ($\sim 0.5\mu\text{M}$) by the metalimnion (figure 4.7a, d). These results are presented in more detail in Corey Goad's thesis (2017)

but are presented here for discussion of key OCC within BML. This observed result differs from those observed in tailings ponds where methane oxidation has been documented to occur in the surface waters but is restricted in the deeper waters due to anoxia (Saidi-Mehrabad et al., 2012). FIS determined surface FFT pore water NH_4^+ concentrations of $\sim 225\mu\text{M}$ decreased significantly above the FFT (ANOVA, d.f= 2, $p < 0.05$; Figure 4.7e) to $< 50\mu\text{M}$ within the first 30 cm of the overlying water. NH_4^+ persisted higher up in the water cap, but at lower concentrations, $\sim 10\mu\text{M}$ in the oxygenated layers (epilimnion + metalimnion) (figure 4.7b, e). These NH_4^+ concentrations are much lower than those observed in tailings pond water cap concentrations of $\sim 700\mu\text{M}$ (Stasik et al., 2014). NH_4^+ concentrations are lower in BML for at least two reasons. One, there is no continuous addition of FFT which would provide ongoing inputs of NH_4^+ in to the water cap, thus water cap concentrations are due to mobilization from the underlying FFT layer within BML as well as any possible denitrification that may be occurring within the water cap. However, the water cap does remain oxic to the FWI indicating that aerobic metabolisms should extend throughout the entire water column. Second, results are consistent with the establishment of nitrifiers and their redox transformation of NH_4^+ to NO_2^- or NO_3^- in BML (Risacher et al., 2017). FIS determined concentrations of $\Sigma\text{H}_2\text{S}$ extinguished rapidly above the FWI, from $\sim 25\mu\text{M}$ in the surface FFT to $< 5\mu\text{M}$, 30cm above the FWI and non-detectable concentrations occurred above this depth (Figure 4.7c, f), consistent with rapid abiotic oxidation in an oxygenated water cap (Luther et al., 2011).

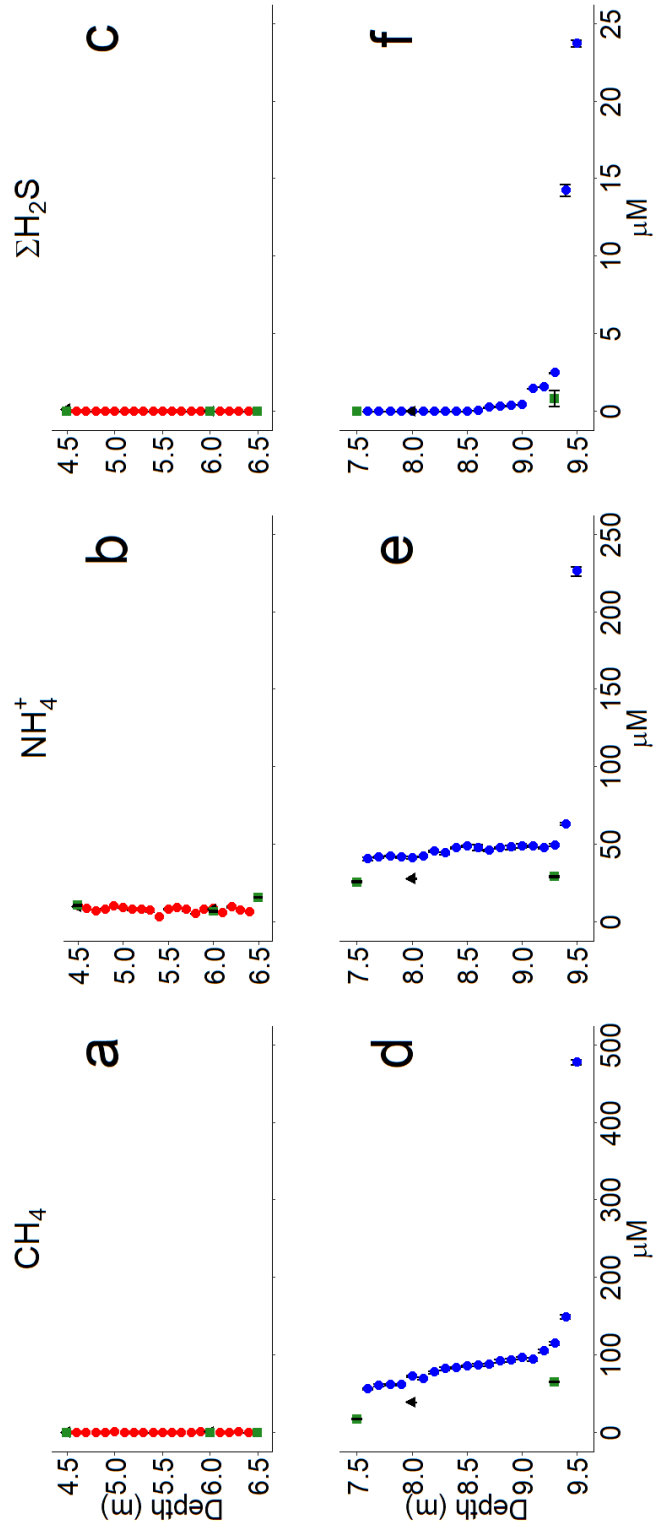


Figure 4.7- FIS generated OCC geochemical data of the BML water cap metalimnetic (n=20; red) and hypolimnetic-FWI (n=20;blue) zones. Green squares represent August 4, 2016 data, while black triangles represent August 13, 2016.

4.5 Hypolimnetic and Metalimnetic OCC vs Oxygen Concentration relationships

The FIS results indicate the presence of both CH₄ and NH₄⁺ in to the overlying water cap; albeit at differing rates of decrease away from the FWI and differing depths to which they penetrate up in to the water cap (Figure 4.7a,b,d,e). To determine their relative importance in driving observed oxygen concentrations within the hypolimnetic and metalimnetic regions, linear regression analysis was used. FIS generated CH₄ and NH₄⁺ concentrations versus water cap oxygen concentrations were modeled to assess their roles in decreasing oxygen concentrations within both regions of the BML water cap.

Methane concentrations were moderately negatively correlated with oxygen concentrations in the metalimnion (Figure 4.8a; $r^2=0.55$, d.f.=19, $p<0.01$) and strongly negatively correlated in the hypolimnion (Figure 4.8b; $r^2= 0.95$, d.f.=17, $p<0.001$); however, the impact was greater in the hypolimnetic region closest to the FWI, where CH₄ concentrations were highest, as identified by a higher r^2 and much lower p-value, indicating the O₂ loss is better explained by CH₄ in this zone (Figure 4.8b). Methane has been shown to be an important negative driver of oxygen concentrations within oil sands tailings ponds (Saidi-Mehrabad et al., 2012). However, in oil sands tailings ponds, this impact is restricted to the shallow surface waters (<1m) that are oxic. The BML results shown here indicate the penetration of O₂ to the FWI (Figure 4.6; ~9.5m) signifying that the chemical oxygen demand (COD) and biological oxygen demand (BOD) of BML, at least in early stage development, are lower than those occurring within tailings ponds.

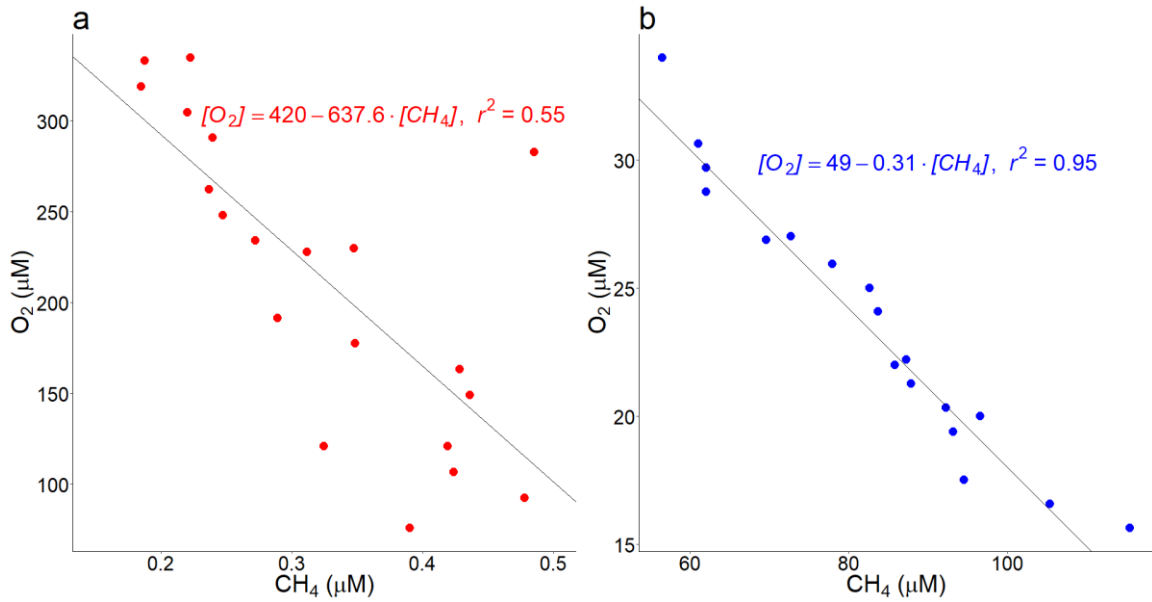


Figure 4.8- Linear regression models of FIS CH_4 concentrations versus oxygen in the metalimnetic region (a; $n=20$) and hypolimnetic-FWI region (b; $n=18$).

In contrast to the results identifying a strong negative relationship between CH_4 and O_2 concentrations within both zones, no statistically significant relationship was observed between NH_4^+ and O_2 within the metalimnion, despite the higher NH_4^+ concentrations relative to other OCC found in this portion of the BML water cap (Figure 4.9a; $r^2=0.008$, d.f.=19, $p>0.05$). A significant negative relationship was only observed between NH_4^+ and O_2 in the hypolimnion (Figure 4.9b; $r^2= 0.81$, d.f.=17, $p<0.01$).

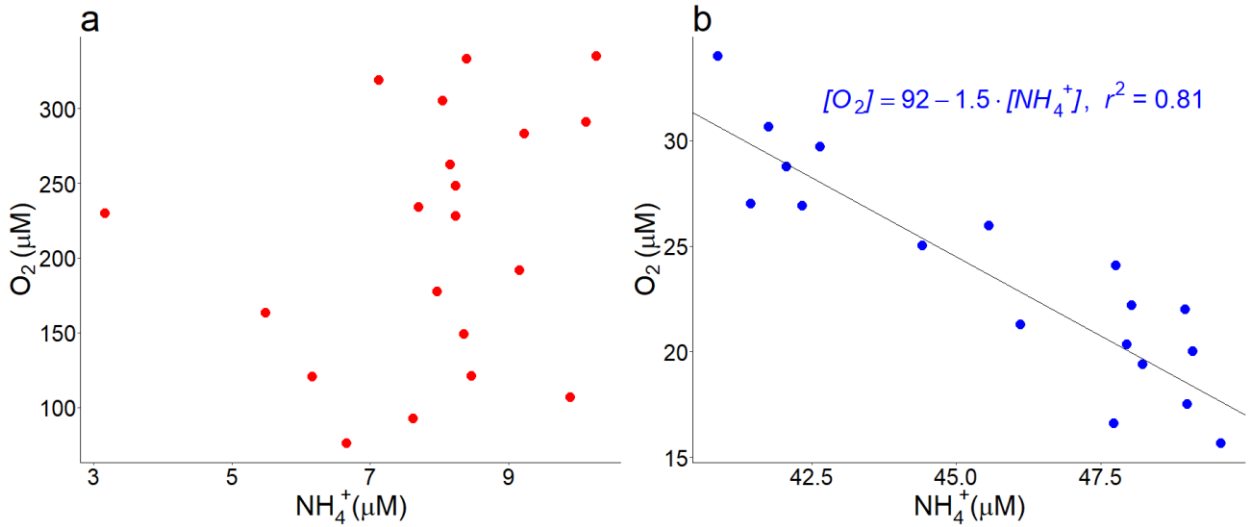


Figure 4.9- Linear regression models of FIS NH_4^+ concentrations ($n=20$) versus oxygen in the metalimnetic region (a; $n=20$) and hypolimnetic-FWI region (b; $n=18$).

4.6 Nitrification within the BML water cap

The process of nitrification is carried out by two distinct genera of microbe, the first step, oxidation of NH_4^+ to NO_2^- is carried out by *Nitrosomonas spp.* While the second step, of NO_2^- to NO_3^- , is carried out by *nitrobacter spp.*, and has a 200kJ/mol lower energy yield (ΔG) than that of the first step (Collins et al., 2016; Roy & Knowles, 1994; Small et al., 2013).

As previously mentioned, NH_4^+ has not been documented to contribute to oxygen loss in tailings ponds though it is abundant and widespread constituent in oil sands FFT (Saidi-Mehrabad et al., 2012; Stasik et al., 2014). It has been hypothesized that nitrification is impeded by the NA toxicity, and a concentration of 80 mg/L has been

suggested as a lower limit at which this toxicity shuts down this microbial process (Misiti et al., 2013; Quagraine et al., 2005).

In BML, the results from 2016 are consistent with active microbial nitrification occurring, which was not observed in 2015 (Figures 4.10 and 4.11, Risacher et al., 2017). A comparison of the associated concentrations and relative proportions of the three nitrogen species in the hypolimnetic and metalimnetic regions from the FIS sampling (and van Dorn sampling for dates bracketing the FIS sampling) are shown in figures 4.10 and 4.11. These figures indicate that O₂ limitation drives microbial nitrification in BML. In the hypolimnion, where O₂ concentrations are <5%, not much conversion of NH₄⁺ to NO₃⁻ is seen (Figure 4.10 and 4.11), however once in the metalimnion, the NH₄⁺ that was found in the hypolimnion has been converted to NO₃⁻. There is a striking contrast between the concentrations and relative proportions of the two end members NH₄⁺ and NO₃⁻ between the hypolimnion and metalimnion, where in the hypolimnion 75% of the total nitrogen species is NH₄⁺ where O₂ is limited (<5% saturation) (Figure 4.11). However, once in the metalimnion ~75% of the total nitrogen species is NO₃⁻ where O₂ concentrations are higher (>10% saturation) (figure 4.11). These results are strongly supportive of active microbial nitrification occurring in BML and that O₂ concentrations govern the extent of this process.

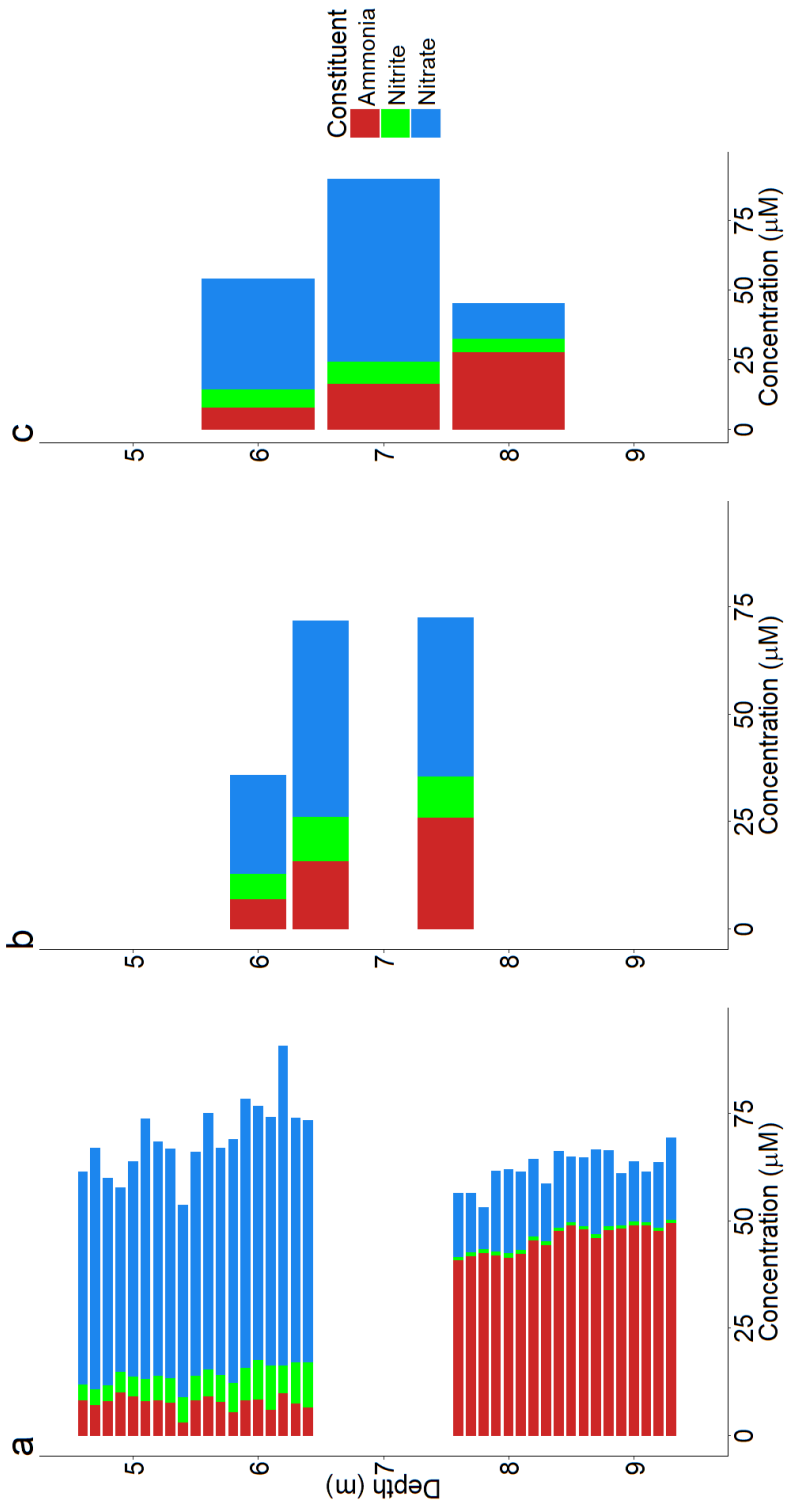


Figure 4.10- stacked bar chart depth profiles of total nitrogen species for FIS (a), as well as the weekly geochemical sampling data surrounding the FIS sampling, August 4 (b) and August 13 (c).

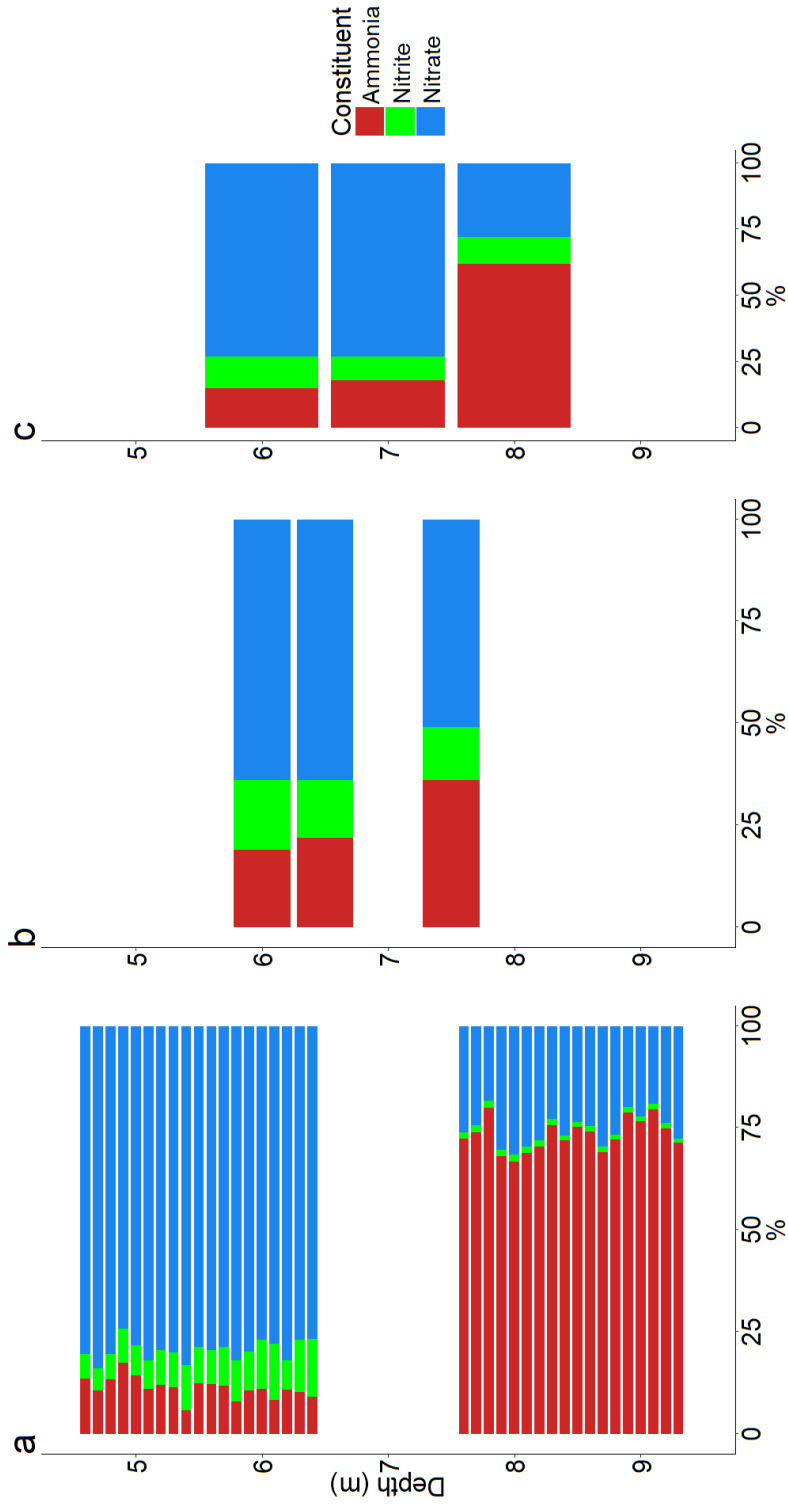


Figure 4.11 - Stacked bar chart of relative proportion depth profiles of nitrogen species for FIS (a), as well as the weekly geochemical sampling data surrounding the FIS sampling, August 4 (b) and August 13 (c).

Further, figure 4.10a and 4.11a show an increase in the concentration and proportion of NO_2^- from the hypolimnion ($<1\mu\text{M}$; $<1\%$) to the metalimnion ($\sim 5\mu\text{M}$; $\sim 10\%$). The metalimnetic-hypolimnetic boundary, found between 6.5-7.5m, where the increase in NO_2^- likely takes place is the same region where O_2 saturation begins to increase (10-15%; figure 4.6). It is likely that the higher O_2 concentrations in the metalimnion enable greater oxidation to occur not only to NO_2^- but also to NO_3^- (Rysgaard et al., 1994). Although the first step of nitrification has a greater energy yield than the second, the limited O_2 concentrations within the hypolimnion likely impede the nitrifying bacteria to actively metabolize.

Moreover, a comparison of the total nitrogen concentrations from the metalimnion and the hypolimnion show they are within 5% of each other. While denitrification has been shown to produce N_2 and N_2O gas in both freshwater and coastal marine systems (Rysgaard et al., 1994; Seitzinger, 1988), our data suggests the loss of nitrogen in BML is insubstantial.

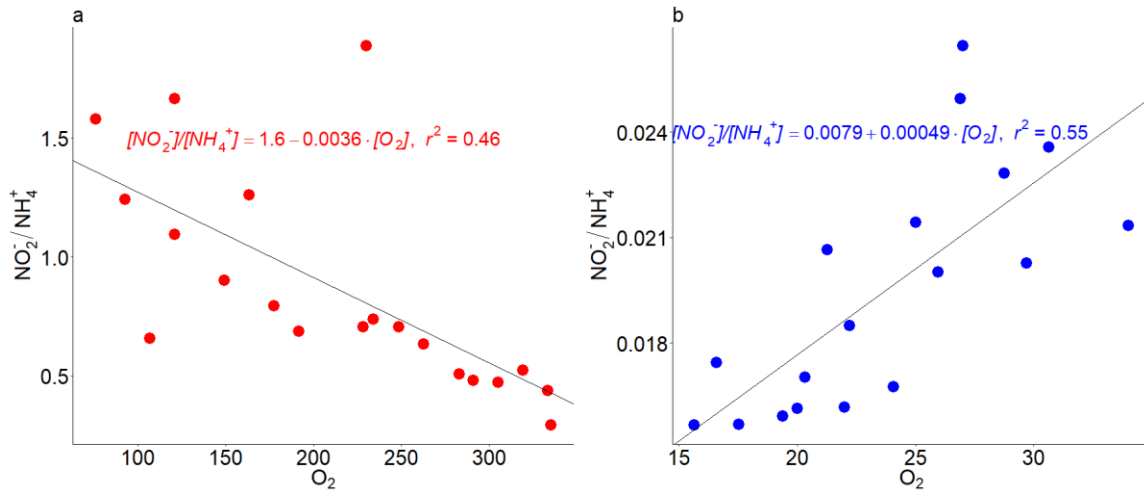


Figure 4.12- High resolution linear regression modelling of NH_4^+ conversion to NO_2^- in the metalimnion (red; a) and hypolimnion (blue; b).

Modelling O_2 vs. NO_2^- / NH_4^+ in the metalimnion (4.12a) revealed a weak negative correlation ($r^2=0.46$, $p<0.05$) while the hypolimnion revealed a moderate positive correlation in the hypolimnion ($r^2=0.55$, $p<0.05$; Figure 4.12b). Where O_2 is limiting ($<20\mu M$), closer to the FWI the ratio of NO_2^- / NH_4^+ is smaller, however as O_2 starts to increase (moving away from the FWI) this ratio also increases, indicating a greater relative oxidation of NH_4^+ to NO_2^- and suggesting that this microbial process is sensitive to oxygen concentrations (figure 4.12b). This result combined with the results showing the similar change in proportions of $NH_4^+/NO_2^-/NO_3^-$ throughout the hypolimnetic and metalimnetic region (figure 4.11) imply that once a threshold of O_2 concentrations is reached, the nitrifiers are able to become active quickly. The relationship observed in the metalimnion, that is, relatively less NO_2^- compared to NH_4^+ moving up in to the metalimnion where O_2 concentrations are higher (figure 4.12a),

reflects greater relative oxidation of NO_2^- to NO_3^- as the oxygen concentrations increase (Figure 4.13a; $r^2=0.64$, $p<0.05$). Consistent with the notion that there is an oxygen concentration minimum required, especially for the second, less energetically favourable oxidation step, no evidence of the conversion of NO_2^- to NO_3^- in the hypolimnion where O_2 is $<30\mu\text{M}$ was observed (figure 4.13b, $p>0.05$).

Evidence suggests O_2 availability governs nitrifiers in BML with different steps of nitrification occurring in different zones of the BML water cap. These results have shown that NH_4^+ oxidation to NO_2^- likely occurs at the metalimnetic-hypolimnetic boundary and to a lesser extent in the hypolimnion, while the oxidation of NO_2^- to NO_3^- is restricted to oxygenated zones $>90\mu\text{M}$ O_2 . However, another factor that differs between the two regions is the concentration of CH_4 . In the deeper waters and FWI region of the BML water cap, there is little O_2 ($<5\%$ saturation; $<30\mu\text{M}$), and maximum CH_4 concentrations ($\sim 120\mu\text{M}$), while in the metalimnetic region O_2 saturation increases $>10\%$ ($>90\mu\text{M}$) at the lower hypolimnetic-metalimnetic boundary up to $\sim 50\%$ ($\sim 300\mu\text{M}$) at the shallowest depth sampled by FIS and CH_4 concentrations are $<1\mu\text{M}$ within this zone. Thus, methanotrophy may be an important factor in determining where nitrification occurs within the BML water cap. Similarly, the highest concentrations of $\Sigma\text{H}_2\text{S}$ occur at the FWI, rapidly extinguishing above this region (Figure 4.7f). Thus, within the lower hypolimnion and FWI region, closest to the source of OCC, oxygen consumption will be highest, similar to what has been demonstrated in tailings ponds as the highest rates of CH_4 oxidation (O_2 consumption) occur in the deeper surface layer where O_2 can penetrate the furthest (closest to the source of OCC) (Saidi-Mehrabad et al., 2012).

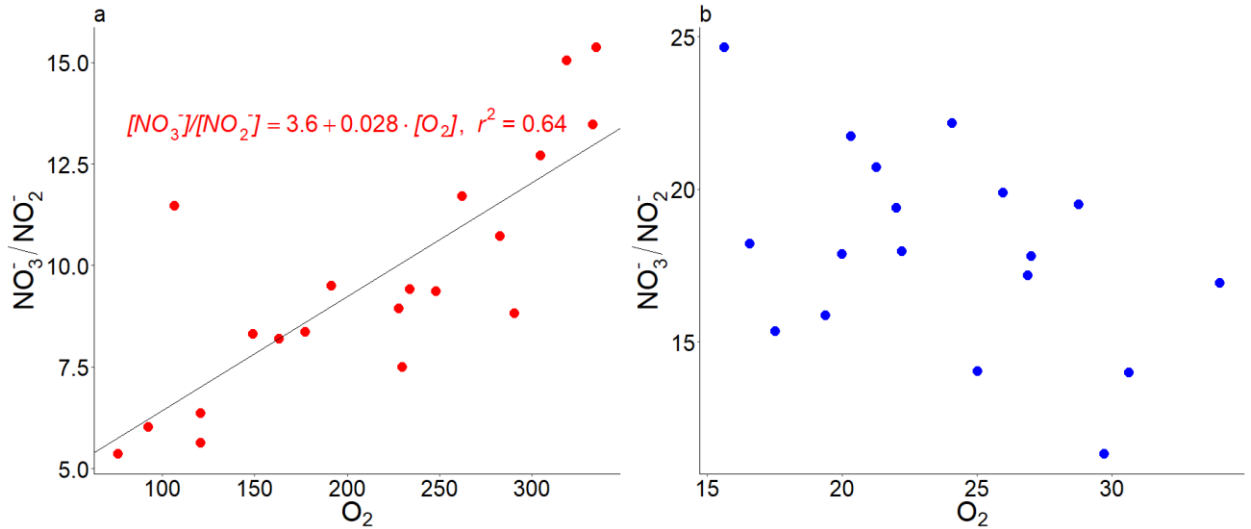


Figure 4.13- High resolution linear regression modelling of NO_2^- conversion to NO_3^- in the metalimnion (red; a) and hypolimnion (blue; b).

In order to assess the possibility that oxygen limitation between methanotrophs and nitrifiers was occurring in BML, linear regression modelling was used.

4.7 Competition between Methanotrophs vs. Ammonia Oxidizers

Methane has been shown to be a competitive inhibitor of ammonia oxidation in freshwater ecosystems by various studies under limiting O_2 concentrations (Carini et al., 2003; Roy & Knowles, 1994; Zheng et al., 2014) and Risacher et al, 2017 has suggested the occurrence of this competition in BML. Evidence from high resolution (FIS) regression modelling supports the occurrence of this process in the hypolimnion of BML (figure 4.14). Figure 4.14a, shows higher concentrations of CH_4 suppress the ability of

ammonia oxidizers to carry out the first step of nitrification in the hypolimnion where O_2 concentrations remain $<30\mu M$ ($r^2 = 0.55$, $p < 0.05$). As concentrations of CH_4 decrease, i.e. moving up in to the water cap away from the FWI, the conversion of NH_4^+ to NO_2^- increases. Once in the metalimnion (figure 4.14b, $r^2 = 0.22$, $p > 0.05$) no evident relationship between the NO_2^-/NH_4^+ and CH_4 concentrations occurs, i.e. higher up in the water column there is more O_2 ($>10\%$ saturation) and little CH_4 ($<1\mu M$) removing the potential restriction on nitrifiers and showing that they are also outcompeted by methanotrophs in BML.

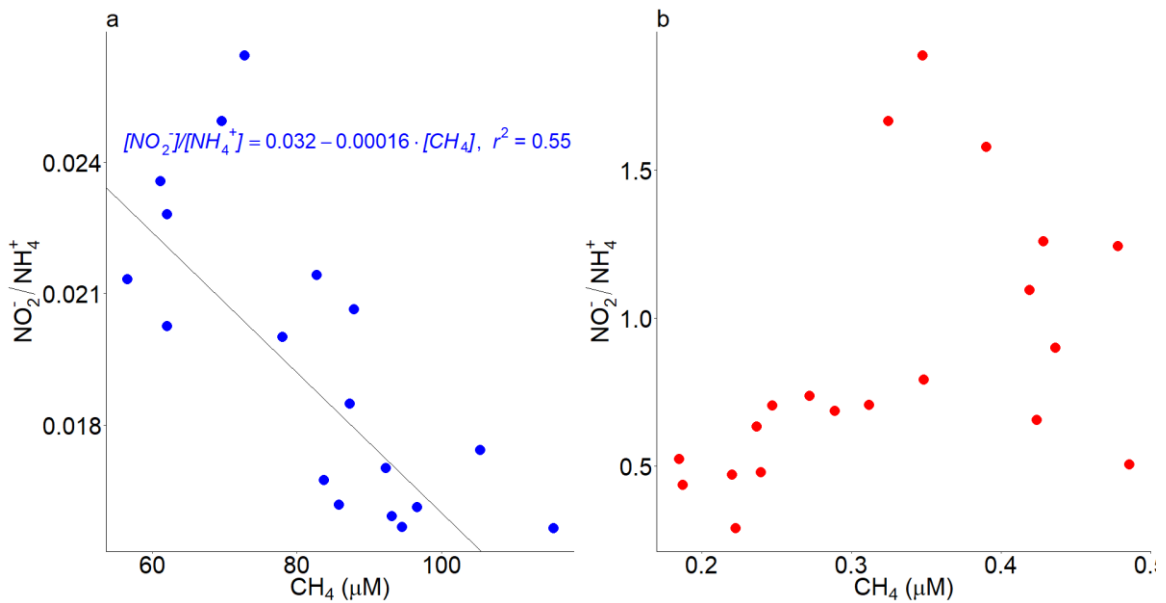


Figure 4.14- High resolution linear regression modelling of CH_4 vs. NH_4^+ conversion to NO_2^- in the hypolimnion (blue; a) and metalimnion (red; b).

4.8 $\Sigma\text{H}_2\text{S}$, NH_4^+ and CH_4 Contribution to Oxygen Depletion in the BML hypolimnion/FWI

Given that $\Sigma\text{H}_2\text{S}$ extinguished rapidly above the FFT its relationship to O_2 in the water cap could not be modelled. However, $\Sigma\text{H}_2\text{S}$, NH_4^+ and CH_4 oxidation will deplete O_2 in the hypolimnion, as such a mass balance was conducted to estimate the impact of these OCC on O_2 in BML in the hypolimnion/FWI.

$\Sigma\text{H}_2\text{S}$ decreases $\sim 23\mu\text{M}$ within the first 40cm above the FFT likely via rapid abiotic oxidation (Luther et al., 2011). This translates to $\sim 55000\text{mol}$ of O_2 needed for oxidation of $\Sigma\text{H}_2\text{S}$ between the first two zones above the FFT (figure 4.15), calculated using the volume of water in each 0.5m zone of BML (Data provided by UBC) and $\Sigma\text{H}_2\text{S}$ concentrations from the FIS. By comparison, over the same two zones NH_4^+ would require $\sim 250000\text{mol}$ and CH_4 requiring $\sim 610000\text{mol}$ of O_2 (Figures 4.16 and 4.17) for the oxidation of these OCC in that layer. While these values are estimates, their general values can be interpreted. As $\Sigma\text{H}_2\text{S}$ is extinguished rapidly above the FFT, its influence on oxygen is restricted to the lower hypolimnion. By comparison, the amount of O_2 needed for $\Sigma\text{H}_2\text{S}$ oxidation is only a fraction ($\sim 20\%$) of what is needed for the oxidation of the other OCC, it is likely CH_4 and NH_4^+ contribute more significantly to the O_2 loss found in BML.

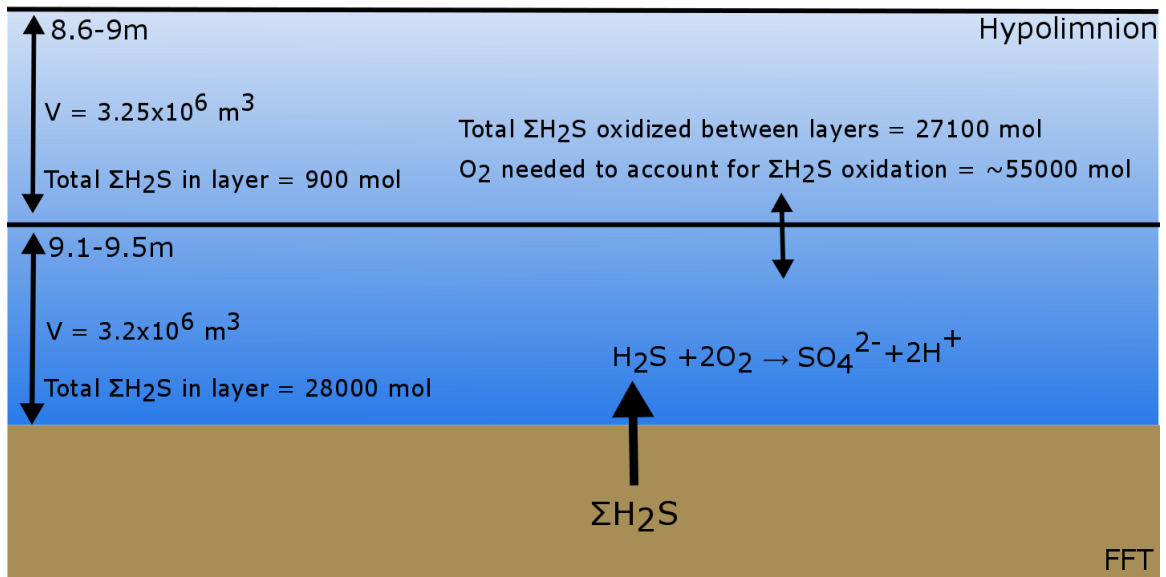


Figure 4.15- simplified schematic of mass balance calculations used to determine $\Sigma\text{H}_2\text{S}$ impact on BML O_2 .

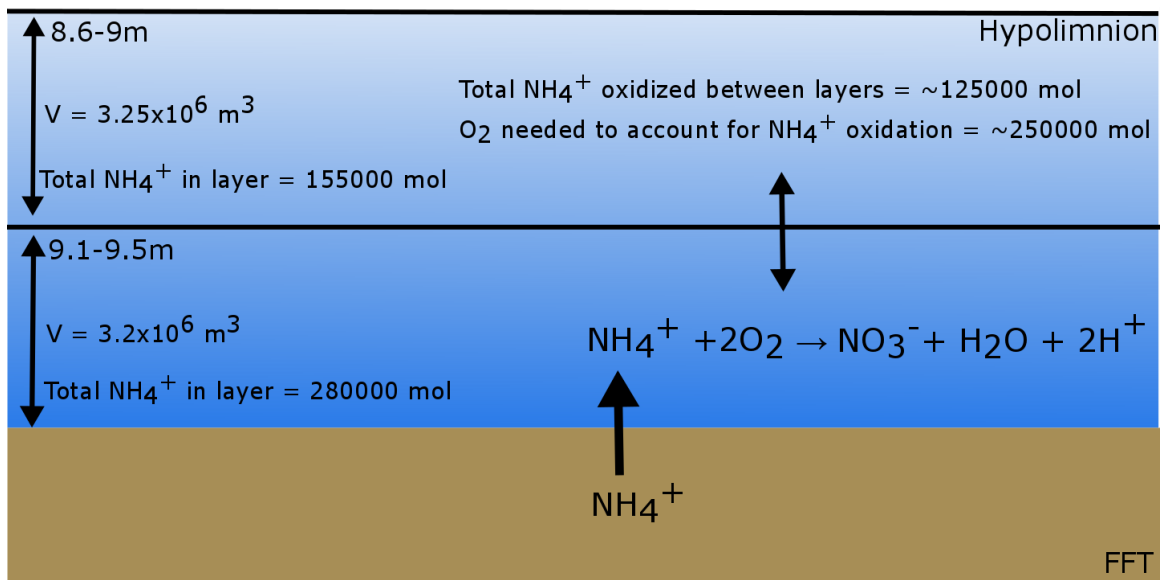


Figure 4.16- simplified schematic of mass balance calculations used to determine NH_4^+ impact on BML O_2 .

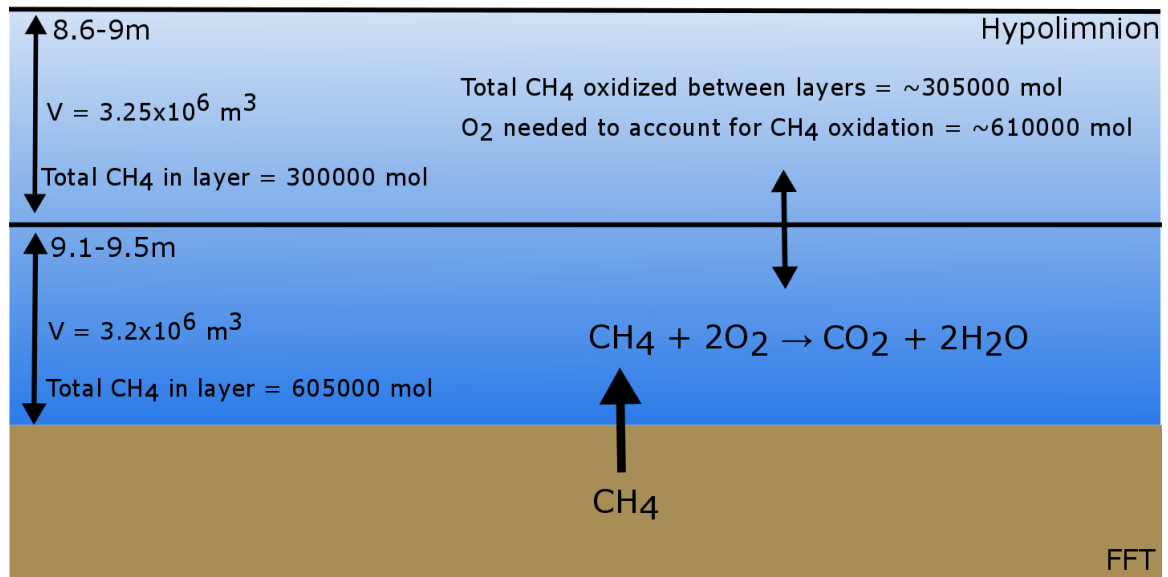


Figure 4.17- simplified schematic of mass balance calculations used to determine CH_4 impact on BML O_2 .

Chapter 5- Conclusion

5.0 Conclusion

This study identified the source of OCC (CH_4 , NH_4^+ and $\Sigma\text{H}_2\text{S}$) in to the BML water cap to be the FFT layer beneath as shown to be the case in tailings ponds. However, unlike a tailings pond BML exhibited an oxic water cap down to the FWI ($<30\mu\text{M}$) where the most intense redox cycling occurred. High resolution geochemical characterization identified that methanotrophy occurred throughout the FWI in to the hypolimnion where oxygen was limited and CH_4 reached trace concentrations once in the metalimnion and above. NH_4^+ oxidation occurred in the FWI and metalimnetic-hypolimnetic boundary, with little activity detected throughout the hypolimnion. This is likely explained by two main reasons, first oxygen limitation governs the two-step nitrification process, while second, methanotrophy likely outcompetes nitrifiers at low O_2 conditions. Unlike in a tailings pond, BML has shown to have nitrification occurring in the water column within the first four years post-commission. $\Sigma\text{H}_2\text{S}$ was detected in the FWI and lower hypolimnion but is oxidized quickly in the oxygenated water cap. Results have revealed a depth dependant importance for all three OCC with little oxidation found to occur in the upper oxygenated layers of BML.

The emergence of competition between methanotrophs and ammonia oxidizers under limited O_2 conditions in conjunction with relatively high FFT pore water concentrations for all three OCC suggests that their subsequent redox biogeochemical processes will impact BML hypolimnetic water cap O_2 concentrations for decades.

However, the summer stratified and oxygenated water cap of BML have proven to restrict a large portion of the oxygen consumption of OCC to the FWI and hypolimnion with only a small fraction of OCC reaching the metalimnion and above. Results have shown that the impact of oxygen consumption from all three OCC is much greater in the hypolimnion/FWI where their concentrations are higher and oxygen is limited. Therefore, the upper water layers of BML may eventually be suitable for macroscopic life.

Further, the emergence of nitrification in BML as well as methanotrophy having been shown to occur in the deeper oxygenated zones of BML, it is likely that the NA toxicity as well as both the COD and BOD are lower than that observed in tailings ponds. With these results being encouraging with respect to tailings pond findings, pit lakes are a promising WCTT.

However, while BML has generated some positive results in the direction of a viable WCTT it is still in early stages of development. BML has exhibited both physico-chemical and biogeochemical discrepancies that differ in relevance and magnitude to those documented in tailings ponds, as such the research done on these tailings ponds cannot be solely relied upon to determine the viability of pit lakes as a wet reclamation strategy. Pit lakes are likely to increase in relevance as a wet reclamation strategy in the AOSRC with ~30 pit lakes awaiting permitting, as such it is critical to understand the biogeochemical processes that will impact a PL to inform the design of future WCTT.

6.0 References

- Arkell, N., Kuznetsov, P., Kuznetsova, A., Foght, J. M., & Siddique, T. (2015). Microbial Metabolism Alters Pore Water Chemistry and Increases Consolidation of Oil Sands Tailings. *Journal of Environment Quality*, 44(1), 145.
<https://doi.org/10.2134/jeq2014.04.0164>
- BGC Engineering. (2010). *Review of Reclamation Options for Oil Sands Tailings Substrates*.
- Boehrer, B., & Schultze, M. (2008). Stratification of lakes. *Reviews of Geophysics*, 46(2), RG2005. <https://doi.org/10.1029/2006RG000210>
- Carey, S. (2008). Growing season energy and water exchange from an oil sands overburden reclamation soil cover, Fort McMurray, Alberta, Canada. *Hydrological Processes*, 22, 2847–2857.
- Carini, S., Bano, N., LeCleur, G., & Joye, S. B. (2005). Aerobic methane oxidation and methanotroph community composition during seasonal stratification in Mono Lake, California (USA). *Environmental Microbiology*, 7(8), 1127–1138.
<https://doi.org/10.1111/j.1462-2920.2005.00786.x>
- Carini, S., Orcutt, B., & Joye, S. (2003). Interaction between methane oxidation and nitrification in coastal sediments. *Geomicrobiology Journal*, 20, 355–374.
- CEMA. (2007). *End pit lakes technical guidance document*.
- Chen, M., Walshe, G., Fru, E., Ciborowski, J., & Weisener, C. (2013). Microcosm assessment of the biogeochemical development of sulfur and oxygen in oil sands

fluid fine tailings. *Applied Geochemistry*, 37, 1–11.

Collins, C. E. V., Foght, J. M., & Siddique, T. (2016). Co-occurrence of methanogenesis and N₂ fixation in oil sands tailings. *Science of the Total Environment*, 565, 306–312. <https://doi.org/10.1016/j.scitotenv.2016.04.154>

David Bastviken, *, †, Jörgen Ejlertsson, † and, & Tranvik‡, L. (2002). Measurement of Methane Oxidation in Lakes: A Comparison of Methods. *Environ. Sci. Technol.*, 36(15), 3354–3361. <https://doi.org/10.1021/ES010311P>

Dompierre, K. A., Lindsay, M. B. J., Cruz-Hernandez, P., & Halferdahl, G. M. (2016). Initial geochemical characteristics of fluid fine tailings in an oil sands end pit lake. *Science of the Total Environment*, 556, 196–206. <https://doi.org/10.1016/j.scitotenv.2016.03.002>

Fedorak, P. M., Coy, D. L., Dudas, M. J., Simpson, M. J., Renneberg, A. J., & MacKinnon, M. D. (2003). Microbially-mediated fugitive gas production from oil sands tailings and increased tailings densification rates. *Journal of Environmental Engineering and Science*, 2(3), 199–211. <https://doi.org/10.1139/s03-022>

Garcia, J.-L., Patel, B. K. ., & Ollivier, B. (2000). Taxonomic, Phylogenetic, and Ecological Diversity of Methanogenic Archaea. *Anaerobe*, 6(4), 205–226. <https://doi.org/10.1006/anae.2000.0345>

Goad, C. (2017). *Methane biogeochemical over seasonal and annual scales in an oil sands tailings pit lake*. M.Sc. Thesis.

Harner, N. K., Richardson, T. L., Thompson, K. A., Best, R. J., Best, A. S., & Trevors, J. T. (2011). Microbial processes in the Athabasca Oil Sands and their potential

- applications in microbial enhanced oil recovery. *Journal of Industrial Microbiology & Biotechnology*, 38(11), 1761–1775. <https://doi.org/10.1007/s10295-011-1024-6>
- Headley, J. V., & McMartin, D. W. (2004). A review of the occurrence and fate of naphthenic acids in aquatic environments. *Journal of Environmental Science and Health. Part A, Toxic/hazardous Substances & Environmental Engineering*, 39(8), 1989–2010. Retrieved from <http://www.ncbi.nlm.nih.gov/pubmed/15332664>
- Holowenko, F. M., MacKinnon, M. D., & Fedorak, P. M. (2000). Methanogens and sulfate-reducing bacteria in oil sands fine tailings waste. *Canadian Journal of Microbiology*, 46(10), 927–937. <https://doi.org/10.1139/w00-081>
- King, H., Walters, C., Horn, W., Zimmer, M., Heines, M., Lamberti, W., ... Macleod, G. (2014). Sulfur isotope analysis of bitumen and pyrite associated with thermal sulfate reduction in reservoir carbonates at the Big Piney–La Barge production complex. *Geochimica et Cosmochimica Acta*, 210–220.
- Lawrence, G. A., Tedford, E. W., & Pieters, R. (2016). Suspended solids in an end pit lake: potential mixing mechanisms. *Canadian Journal of Civil Engineering*, 43(3), 211–217. <https://doi.org/10.1139/cjce-2015-0381>
- Luther, G. W., Findlay, A. J., MacDonald, D. J., Owings, S. M., Hanson, T. E., Beinart, R. A., & Girguis, P. R. (2011). Thermodynamics and kinetics of sulfide oxidation by oxygen: A look at inorganically controlled reactions and biologically mediated processes in the environment. *Frontiers in Microbiology*, 2(APR), 1–9. <https://doi.org/10.3389/fmicb.2011.00062>
- Masliyah, J., Zhou, Z. J., Xu, Z., Czarnecki, J., & Hamza, H. (2008). Understanding

Water-Based Bitumen Extraction from Athabasca Oil Sands. *The Canadian Journal of Chemical Engineering*, 82(4), 628–654. <https://doi.org/10.1002/cjce.5450820403>

Misiti, T., Tandukar, M., Tezel, U., & Pavlostathis, S. G. (2013). Inhibition and biotransformation potential of naphthenic acids under different electron accepting conditions. *Water Research*, 47(1), 406–418. <https://doi.org/10.1016/j.watres.2012.10.019>

Mohamad Shahimin, M. F., Foght, J. M., & Siddique, T. (2016). Preferential methanogenic biodegradation of short-chain n-alkanes by microbial communities from two different oil sands tailings ponds. *Science of the Total Environment*, 553, 250–257. <https://doi.org/10.1016/j.scitotenv.2016.02.061>

Penner, T. J., & Foght, J. M. (2010). Mature fine tailings from oil sands processing harbour diverse methanogenic communities. *Canadian Journal of Microbiology*, 56(6), 459–70. <https://doi.org/10.1139/w10-029>

Pramanik, S. (2016). Review of Biological Processes in Oil Sands – A Feasible Solution for Tailings Water Treatment. *Environmental Reviews*, 24(3), 274–284. <https://doi.org/10.1139/er-2015-0088>

Quagraine, E. K., Peterson, H. G., & Headley, J. V. (2005). In situ bioremediation of naphthenic acids contaminated tailing pond waters in the athabasca oil sands region—demonstrated field studies and plausible options: a review. *Journal of Environmental Science and Health. Part A, Toxic/hazardous Substances & Environmental Engineering*, 40(3), 685–722. Retrieved from <http://www.ncbi.nlm.nih.gov/pubmed/15756978>

- Ramanathan, G., Sales, C. M., & Shieh, W. K. (2014). Simultaneous autotrophic denitrification and nitrification in a low-oxygen reaction environment. *Water Science & Technology*, 70(4), 729–735. <https://doi.org/10.2166/wst.2014.292>
- Ramos-Padrón, E., Bordenave, S., Lin, S., Bhaskar, I. M., Dong, X., Sensen, C. W., ... Gieg, L. M. (2011). Carbon and sulfur cycling by microbial communities in a gypsum-treated oil sands tailings pond. *Environ Sci Technol*, 45(2), 439. <https://doi.org/10.1021/es1028487>
- Risacher, F., Morris, P., Arriaga, D., Goad, C., Colenbrander-Nelson, T., Slater, G., & Warren, L. (2017). *The interplay of methane and ammonia as key oxygen consuming constituents in early stage development of Base Mine Lake, the first demonstration Oil Sands pit lake.*
- Roden, E. (2012). Microbial iron-redox cycling in subsurface environments. *Biochemical Society Transactions*, 40(6), 1249–1256. <https://doi.org/10.1042/BST20120202>
- Rogers, V. V., Wickstrom, M., Liber, K., & MacKinnon, M. D. (2002). Acute and Subchronic Mammalian Toxicity of Naphthenic Acids from Oil Sands Tailings. *Toxicological Sciences*, 66(2), 347–355. <https://doi.org/10.1093/toxsci/66.2.347>
- Roy, R., & Knowles, R. (1994). Effects of methane metabolism on nitrification and nitrous oxide production in polluted freshwater sediment. *Applied and Environmental Microbiology*, 60(9), 3307–3314.
- Rysgaard, S., Risgaard-Peterson, N., Peter, S., Kim, J., & Peter, N. (1994). Oxygen regulation of nitrification and denitrification in sediments. *Limnology and Oceanography*, 39(7), 1643–1652.

Saidi-Mehrabad, A., He, Z., Tamas, I., Sharp, C. E., Brady, A. L., Rochman, F. F., ...

Dunfield, P. F. (2012). Methanotrophic bacteria in oilsands tailings ponds of northern Alberta. *The ISME Journal*, 7(10), 908–921.

<https://doi.org/10.1038/ismej.2012.163>

Salloum, M. J., Dudas, M. J., & Fedorak, P. M. (2002). Microbial reduction of amended sulfate in anaerobic mature fine tailings from oil sand. *Waste Management & Research*, 20, 162–171. <https://doi.org/10.1177/0734242X0202000208>

Seitzinger, S. P. (1988). Denitrification in freshwater and coastal marine ecosystems: Ecological and geochemical significance. *Limnology and Oceanography*, 33(4), 702–724. <https://doi.org/10.4319/lo.1988.33.4part2.0702>

Siddique, T. †, Phillip M. Fedorak, †, Michael D. MacKinnon, ‡ and, & Julia M. Foght*, †. (2007). Metabolism of BTEX and Naphtha Compounds to Methane in Oil Sands Tailings. *Environ Sci Technol*, 41(7), 2350–2356.

<https://doi.org/10.1021/ES062852Q>

Siddique, T., Kuznetsov, P., Kuznetsova, A., Li, C., Young, R., Arocena, J. M., & Foght, J. M. (2014). Microbially-accelerated consolidation of oil sands tailings. Pathway II: solid phase biogeochemistry. *Frontiers in Microbiology*, 5, 107.

<https://doi.org/10.3389/fmicb.2014.00107>

Siddique, T., Penner, T., Klassen, J., & Foght, J. M. (2012). Microbial Communities Involved in Methane Production from Hydrocarbons in Oil Sands Tailings. *Environmental Science and Technology*, 46, 9802–9810.

Siddique, T., Penner, T., Semple, K., & Foght, J. M. (2011). Anaerobic biodegradation of

longer-chain n-alkanes coupled to methane production in oil sands tailings.

Environmental Science and Technology, 45(13), 5892–5899.

<https://doi.org/10.1021/es200649t>

Small, G. E., Bullerjahn, G. S., Sterner, R. W., Beall, B. F. N., Brovold, S., Finlay, J. C.,

... Mukherjee, M. (2013). Rates and controls of nitrification in a large oligotrophic lake. *Limnology and Oceanography*, 58(1), 276–286.

<https://doi.org/10.4319/lo.2013.58.1.0276>

Stasik, S., Loick, N., Knöller, K., Weisener, C., & Wendt-Potthoff, K. (2014).

Understanding biogeochemical gradients of sulfur, iron and carbon in an oil sands tailings pond. *Chemical Geology*, 382, 44–53.

<https://doi.org/10.1016/j.chemgeo.2014.05.026>

Stasik, S., & Wendt-Potthoff, K. (2014). Interaction of microbial sulphate reduction and

methanogenesis in oil sands tailings ponds. *Chemosphere*, 103, 59–66.

<https://doi.org/10.1016/j.chemosphere.2013.11.025>

Syncrude. (2017). Water Capping. Retrieved June 30, 2017, from

<http://www.syncrude.ca/environment/tailings-management/tailings-reclamation/water-capping/>

Tiedje, J. (1988). Ecology of denitrification and dissimilatory nitrate reduction to

ammonium. *Environmental Microbiology of Anaerobes*, 179–244.

Torres-Alvarado, R., Ramírez-Vives, F., Fernández, F. J., & Barriga-Sosa, I. (2005).

Methanogenesis and methane oxidation in wetlands. Implications in the global

carbon cycle Metanogénesis y metano-oxidación en humedales. Implicaciones en el

ciclo del carbono global. *Hidrobiológica*, 15(3), 327–349. Retrieved from

<http://www.scielo.org.mx/pdf/hbio/v15n3/v15n3a9.pdf>

Viollier, E., Inglett, P. ., Hunter, K., Roychoudhury, A. ., & Van Cappellen, P. (2000).

The ferrozine method revisited: Fe(II)/Fe(III) determination in natural waters.

Applied Geochemistry, 15(6), 785–790. <https://doi.org/10.1016/S0883->

2927(99)00097-9

Zheng, Y., Huang, R., Wang, B. Z., Bodelier, P. L. E., & Jia, Z. J. (2014). Competitive

interactions between methane- and ammonia-oxidizing bacteria modulate carbon

and nitrogen cycling in paddy soil. *Biogeosciences*, 11(12), 3353–3368.

<https://doi.org/10.5194/bg-11-3353-2014>